INDIVIDUAL REPORT – I2

Modelling the response of the built environment to climate change

Review of the Lumped Parameter Model and study of its application to a room in the Engineering building

James Bunting

Candidate Number: 024338

Student Number: 590021680

ECMM102 – Group Project (MEng)

Climate change is predicted to have a significant effect on the built environment in the coming decades. This project aims to model the effects of climate change on built environment such as lecture theatres and the interaction of human occupants within the buildings. In particular with the predicted increase in the use of natural ventilation it is critical to simulate and understand the airflow and internal conditions. A room in the Engineering building (Room 170) is chosen as an experimental test bed upon which the simulations and modelling is based. This report will focus on the development of the Lumped Parameter Model (LPM) which is an electrical analogy of the room. The design of buildings is modelled by resistor-capacitor networks (RC-networks) which are computationally expensive. The LPM reduces these large RC-networks into a few simple networks. The LPM represents multi-layered constructions and is able to simulate the effect of internal and external weather on a built environment. A LPM RC-network will be created for Room 170 and used to model the temperature change within the room. Results of the computational fluid dynamics (CFD) simulation are used to validate the LPM. It is possible to scale up the RCN for a more complex setup such as the entire engineering building. The final aim of the project is to identify how CFD modelling can be used to model the influence of climate change on built environments.

Keywords: CFD, Lumped Parameter Model, building modelling, climate change

Table of Contents

1 Introduction

Climate change is a very present issue: the global temperature is predicted to rise by 1.4-5.8°C by the end of the 21st century.[1] The population of the world is also changing: currently 50% of the world's population live in cities; by 2050 this is predicted to swell to 70%. [2] With these figures in mind it is becoming increasingly important to calculate the effect of climate change on buildings. The ever increasing population of cities and rise in energy prices has encouraged the transition from mechanically driven heating, ventilation and air conditioning HVAC systems to the use of natural ventilation. By its nature, natural ventilation systems are not as controlled or predictable as traditional HVAC systems. There has been much research into the airflow and heat transfer of bodies in a room and the coupling of a CFD simulation with the IESD-Fiala model. The model predicts the thermo-regulatory response from the human body according to the surrounding conditions.

Furthermore, bearing in mind the increasing energy prices and the constant strive for lower "carbon footprints", one of the aspects of building design is energy efficiency. Energy efficient buildings are designed to retain thermal energy in the winter and dissipate excess thermal energy in the summer. Since the building material is not altered on a seasonal basis it is important to be able to construct the building walls with materials that perform well at all times of the year. Choosing a material intelligently means taking into account its thermal retention and irradiative properties. A complicating factor with building construction is the inclusion of occupants; an empty building may perform efficiently in the design stage but never reach its projected energy saving targets once inhabited. The human occupants of a building do not have a constant or regular set of conditions for a comfortable internal environment. The opening and closing of windows, propping open of doors and manual changing of thermostats disrupts the energy performance of a building. For this reason it is important to also combine the material infrastructure of a workspace with the HVAC system. The increasing use of natural ventilation as a part of the HVAC system introduces an element of unpredictability to the system. The control of the natural ventilation plays a large role in the thermal comfort of the occupants.

1.1 The IESD-Fiala Model and the room CFD model

As mentioned earlier there has been previous research into the thermo-regulatory response of the human body, the most prevalent being the development of the IESD-Fiala model. The model was created 15 years ago by Dr Dusan Fiala to model the human thermal responses. The Fiala model can be used for short term i.e. transient simulations and heterogeneous conditions. The variables can also be modified to simulate the human environmental response after a variety of activity levels. The human's response can be in the form of vasodilatation for the onset of sweating or vasoconstriction which leads to shivering. The computer simulation of the human response to environmental factors can be used in a variety of engineering scenarios such as in the modelling of passenger comfort inside a car and the thermal comfort analysis of buildings and individual built components. The model comprises two systems; an active and a passive system. The passive system deals with the constant thermophysical and thermophysiological properties of the human body. This includes the circulation of blood and heat transfer around the tissue. The active system deals with the response of the body to environmental conditions, e.g. sweating and shivering. Through the incorporation of experimental thermal comfort data the Fiala model has been modified to reflect the thermal comfort and human perceived responses to a range of atmospheric conditions. [3]

As much as the coupling of the active and passive systems in the IESD-Fiala model is important for simulating an accurate human response, this is also the case for the coupling of a human thermal comfort model with CFD. Since 2000, much research has been conducted on human thermal model to CFD coupling using a variety of coupling methods. The methods, briefly mentioned in (Cropper et al) [4], cover changes in the human geometry - simplified, male or female; the number of nodes in the thermal regulatory model and even models with moveable limbs. The paper by Cropper [4] is the most recent in the human thermal model to CFD coupling field. The aggregated system functions by two-way data transfer [4]. A CFD simulation is run to develop environmental conditions around the human model; this data is then fed into the thermo regulatory model (in this case the IESD-Fiala model) which generates the appropriate human response and body surface conditions. The data transfer is particularly important when modelling naturally ventilated spaces. In these conditions the air velocities are low and the effect of the human body on the local environment is exaggerated. In this project the same principles of coupling will be used to simulate the reaction and response of a human model placed in a room in the engineering building. The coupled system will be able to provide a better understanding of the influence of building ventilation systems on the occupants and vice versa.

1.2 The Lumped Parameter Model

The coupled system will be used to validate a Lumped Parameter Model (LPM). An LPM will be created to model the heat transfer of room walls and the effect of the surrounding conditions on the internal climate. The LPM is an electrical representation of the walls and surrounding surfaces of a room. It can also be scaled up to represent an entire building. In the case of this report, a model will be created for a specific room in the engineering building; the model will have component properties which represent the structure of the surrounding walls and their material properties. The LPM uses far fewer components and equations than a full model because it is able to produce accurate results for the operating range in a shorter time and at a much lower computational cost. It is also possible to model more complex wall cross sections using the Dominant Layer LPM; this is used more often for exterior walls as they are composed of a variety of different insulating materials. The Dominant Layer model further simplifies the modelling of buildings by focusing on the heaviest layer in a wall cross section. This heaviest layer – the dominant layer – has the largest contribution to the internal gains. Since all changes in layers before the dominant layer are overshadowed by the dominant layer it is possible to ignore the preceding layers. Fewer layers further reduces the computational time and cost variables.

In the previous individual report the details of choosing a suitable room are specified. [5] The room chosen as a test-bed was Room 170 in the Harrison building. Room 170 is totally internal; there are no external walls or windows. This aids the initialisation of the simulation because there is minimal effect from the heterogeneous weather conditions and it is simple to create a stable environment. The room was modelled in SolidWorks; this model could be edited to create a range of room models from a simple version to a complex version. Small extruding objects like the door handles and light switches could be omitted as they played no significant effect on the net airflow in the room and were detrimental to the time required to run a simulation. This CAD model was then imported to ANSYS FLUENT for the CFD simulations. A compatible CAD model of a simple human figure was created in SolidWorks and much effort was spent on generating an accurate mesh with adequate boundary meshing and minimal skewness.

This report will focus on the modelling of the room as a Lumped Parameter Model (LPM). This model is an electrical analogy of the room using resistors and capacitors as the heat transfer and storage elements of each surface. This is a recent addition to the research covered in the group project. For this reason it is not included in the first individual report. As a result a major section of this report will detail the previous research and development of the LPM. The theory of the method will be explained and this will be applied to Room 170. The method is to be used alongside the room and human interaction simulation to confirm and expand on the findings. Experimental data will be collected for use as simulation accuracy validation, the coupled system will model the airflow and heat transfer from individual human bodies and the LPM will model the heat transfer through surfaces and have the future capability of modeling the internal temperatures in response to predicted future climate conditions.

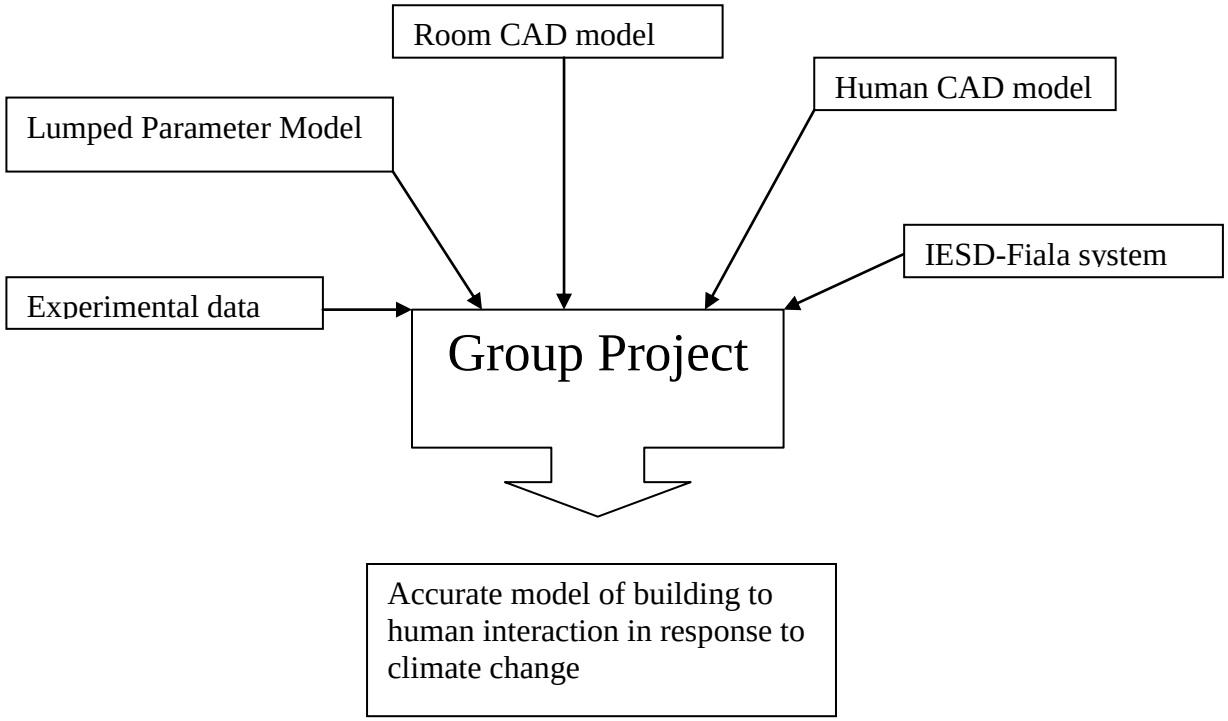

Figure 1: Graphic of the project sub-sections.

2 Literature Review

2.1 Second Order System Identification

The use of a LPM with building modelling for the purpose of reducing efficiency losses has been an area of research since the early 1990s. One paper [6] uses a second order system in the thermal response of buildings to be used for online building energy management and control. The paper describes a recursive least squares algorithm which is used to identify five parameter variables. The system functions using a network of three resistors and two capacitors arranged as shown in the circuit diagram Figure 2.

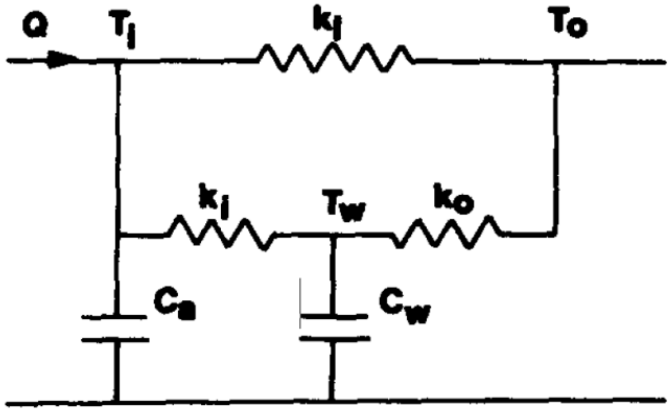

Figure 2: 3R2C network as used in (Coley et al).

Q = heat supply

T_i = inside temperature node

T_o = outside temperature node

T_w = structural temperature node

k_I = quick response thermal conductance

k_i = thermal conductance between T_i and T_w

k_o = thermal conductance between T_w and T_o

C_a = thermal capacity of air

C_w = thermal capacity of building structure

The values for resistance and capacitance are taken manually on site. As opposed to later research which focuses on the use of LPMs for predicting energy efficiency and the interior environment, this paper uses the LPM alongside the general operation of the building. It is designed to run for the lifetime of the building and monitor the energy losses. The system continually updates itself to the current operating performance and highlights any deterioration in building energy efficiency. The paper describes the implementation of an efficient recursive algorithm suitable for Building Energy Management Systems (BEMS) integration. [6]

The RC-Network in Figure 2 simulates heat flow through the walls from inside to outside. The resistor k_i represents wall components which respond quickly to the heat source, i.e. windows, ventilation losses etc. Excluding the k_i resistor and C_a the paper describes the basic building block of all future LPMs; the two resistor one capacitor unit. This unit is used in all later LPM research and can be used to represent any configuration of wall cross section. The circuit can be represented by the following state equations:

$$C_a \frac{dT_i}{dt} = k_i(T_w - T_i) + k_i(T_o - T_i) + q \quad (eq.1)$$

$$C_w \frac{dT_w}{dt} = k_i(T_i - T_w) + k_o(T_o - T_w) \quad (eq.2)$$

Using the state equations, the network is used to plot a convergence of the parameters. The initial conditions are set with experimental values, the system then runs for *k* iterations

calculating the new parameter values based on the values from the previous time step. As *k* increases the estimated value approaches the true value and converges. [6]

The problem with the system is however, that the effects of the previous results continue to have a greater effect on new results than more recent results. The algorithm builds up "inertial drag" for a large *k*. [6] After a large number of time steps the current data has difficulty overcoming the inertial pull of the systems data history. The benefit of the "inertial drag" is that fluctuations in the data are smoothed and rapidly changing data can be processed without difficulty. However, this does make it difficult to monitor slow changing parameters. This problem is resolved by predicting the next data value before its calculation.

2.1.1 OLIVER – The Building Energy Management System

A computer code OLIVER was written for the system to calculate the values of the three resistors and two capacitors. It is possible to modify the code to either follow or ignore slow varying trends by editing the error-covariance matrix. [6] If chosen to follow slow varying trends the matrix restricts the iterations to change by no more than their original value on the first iteration and cannot change by larger values in later iterations.

The results of paper [6] show that k_o, the thermal conductance between the structural temperature node and the outside, was the most difficult variable to identify since it oscillates rapidly before settling. Naturally there is a certain tolerance with the data; overestimation is most likely during warmer days when the calculated maximum is high. The parameter set produces above-average values because it does not consider the human to building interaction: by opening and closing windows or manually changing the ventilation settings, the occupants lower the actual temperature. There is also difficulty in extracting accurate night time minimum temperatures since these tend to be underestimated.

Unlike later systems, OLIVER takes a considerable time (10 days) to converge on accurate values. Over a seven week period, the final parameter set is capable of predicting internal temperatures to within 1°C RMS. This RMS deviation can be reduced by constantly updating the system to actual environmental conditions and predicting only a few hours in the future. Unlike later LPMs the OLIVER system would be used within a functioning building for up-to-date building control.

2.2 A Low-Order System including the Heating System

The paper (Gouda et al)[7] takes a slightly different approach to (Coley et al)[6] in that rather than developing a passive low-order system that is driven by the conditions in the room, it runs a simulation in parallel. This is possible because the low-order model includes heating system and solar radiation models. As in (Coley et al)[6], a physical room is chosen to compare to experimental data. The low-order model is created to model the thermal behaviour of an unoccupied but heated north facing room.

At the time of writing, building energy analysis software was used commonly used but it still had many restrictions. The specification of inputs and outputs was restrictive, meaning that the models were sometimes used for situations in which the conditions did not fit the model. There was also difficulty in obtaining results for short timescales (minutes or hours). Furthermore, steady-state component models do not react well to high-frequency impulse inputs. [7] The earlier paper (Coley et al)[6] was able to overcome these issues; by frequently updating the conditions the model was able to predict future

conditions for the next few hours. High-frequency impulse inputs were smoothed by restricting the change in magnitude per iteration. These solutions were possible because the model was based on a low-order LPM. (Gouda et al)[7] further this work as it comprises of a low-order model but includes additional heat sources.

The building model takes into account three factors; the microclimate, casual heat gains and the heating system.[7] The microclimate is the local environment immediately surrounding the room, this includes solar heat gains. Casual heat gains include the warming effect from occupants, lighting, computers, other electrical appliances etc. The heating system consists of the boiler and radiators in the room. The method for selecting a room was similar to the method used in individual report 1 in choosing Room 170. Both rooms were chosen for their location as it had minimal solar radiation effects. Room 170 is in an ideal location in that it has no external walls and therefore experiences no direct solar radiation, The experimental room in (Gouda et al)[7] is north facing so experiences some solar radiation although much less than other possible rooms. Data was collected from both rooms when it was under normal operating conditions but unoccupied.

The paper [7] details the heating system model as two parts; the heat exchanger with its water connections and the control valve. The heat exchanger provides natural convection and radiation; these are lumped together in the model since the local heat exchanger air temperature and the mean room temperature are similar. Details such as the laminar/turbulent flow in the heat exchanger are calculated. A range of values for the water side convection coefficient are included in the heating system model. Later studies [8]-[9] do not include the different convection coefficients for types of flow because the effect on the total flow is negligible. Rather the heat exchanger is simplified and the thermal output is independent of internal fluid flow. On the other hand the paper does treat fabric solar heat gains through walls and roofs as negligible and this assumption is continued to be used in later research [8]-[10]. The valve output to valve position is non-linear; as the valve position approaches 100%, the valve output increases by a faster rate.

2.2.1 The Inclusion of Solar Radiation

Solar radiation has a significant effect on the model and this is complicated by its uncontrollable nature. For this reason it was important to take into account estimations of the diffuse and direct fractions of incident radiation on a horizontal plane. From these estimations two algorithms were used to estimate the incident solar irradiance on a surface at any orientation.[7] Using the solar radiation model, given the time and date, the value of incident solar radiation on any surface of any orientation may be calculated. The effect of solar radiation is omitted in [9] and [10]; in these papers only the temperature is included in the external factors. Despite this, the solar radiation model does show good correlation with measured values although there is a tendency to underestimate.

Even with all the heating system and solar radiation equations and calculations, the model was chosen to be applied when these factors would be minimal. It is also argued that solar radiation and casual heat gains are of limited interest for high-response dynamic modelling because they are slow acting. [7] Figure 3 (next page) shows the complete low-order model. The model uses the basic two resistors, one capacitor building block as covered in (Coley et al)[6] for its LPM. Each of the exterior walls has its own unit, along with units for the floor, ceiling and partitions. This layout is used in the LPM for Room 170 however instead of having a single input value combining casual heat gains to space and plant heat output, the model for Room 170 uses a separate input for each interior surface. This

method allows for the difference in air temperature in areas around electrical appliances such as a projector or computer.

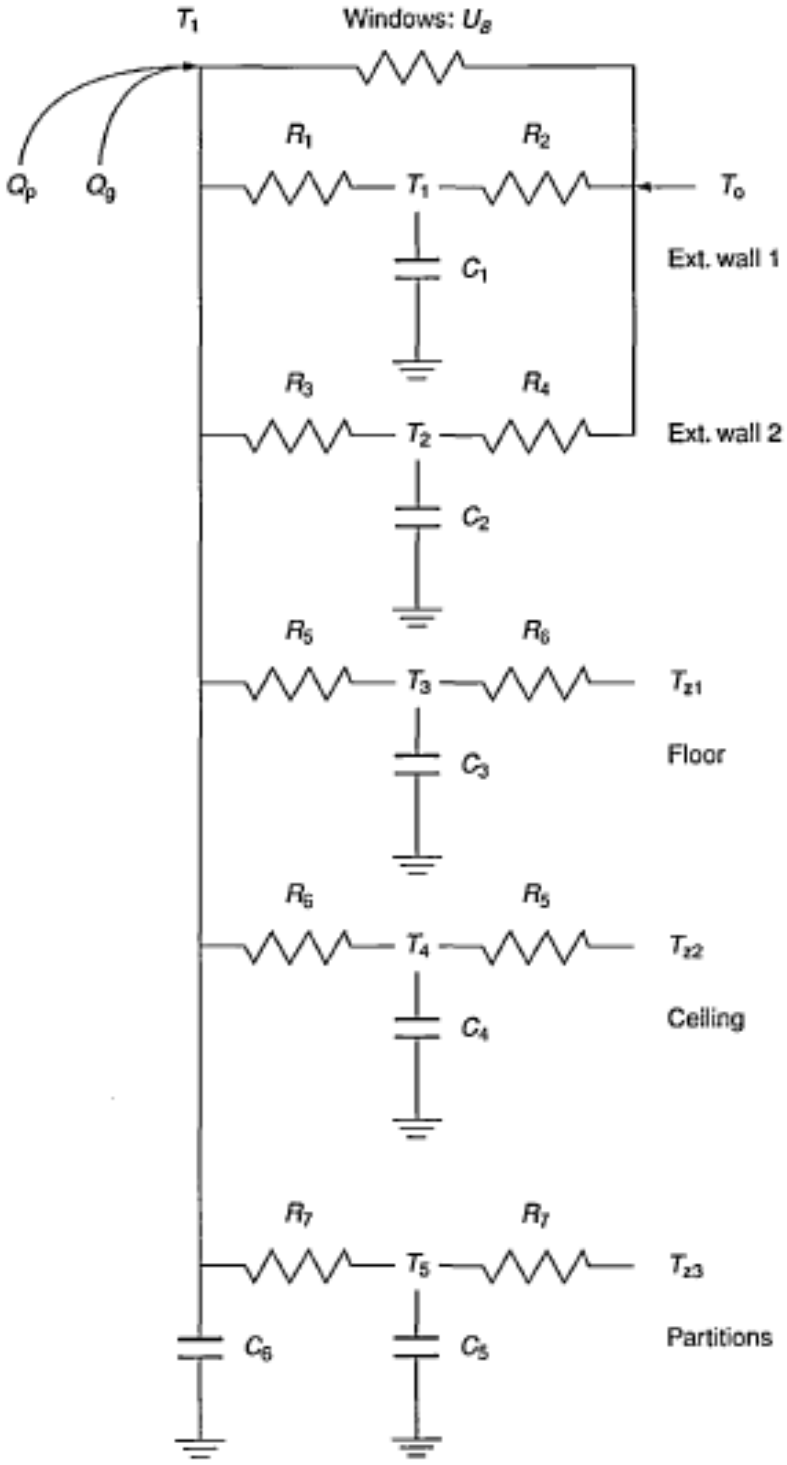

Figure 3: Model realisation for the selected example space.

In accordance with other LPMs the model was validated empirically with experimental results. Experimental data was recorded over several days in order to eliminate any input excitations. During modelling, data was taken at 15 minute intervals over seven days. This is a dramatic improvement compared to the seven week period the OLIVER code required

to predict the internal temperatures. Simulated results showed a very good correlation with measured results. For long term investigation the building envelope mass dominates whereas for short term investigations the room air mass dominates [7] hence why there was such an emphasis on accurate modelling of casual heat gains and solar radiation. In agreement with (Coley et al)[6] the paper specifies that for the model to be accurate, the simple heating system must capture the key low frequency dynamics. In (Gouda et al)[7] this is to be in sync with the dominant air thermal capacity effect and in (Coley et al)[6] this is to correctly follow the slow secular trends such as seasonal differences. The low-order model accurately models short timescale simulations which were not possible with other simulation programs at the time (TRNSYS and DOE). [7] The paper mentions the future possibility of including the influence of occupants on the building analysis system.

2.3 Comparison of three Models: 3R4C, 3R2C and 1R2C

A later paper (Fraisse et al)[8] builds upon the earlier research into low-order building models and introduces the aggregation of walls. The paper compares three different building models; one of three resistors and four capacitors (3R4C), one of three resistors and two capacitors (3R2C) and one of one resistor and two capacitors (1R2C). The reduction of multi-layered constructions into simple single layers is an important step forward in the building modelling sector and is used in later research.[9][10] In a similar direction to the inclusion of the fluid properties of the heating system in Gouda's paper [7], the paper discusses the modelling of a hydraulically heated floor. This models the water-loop in steady state as opposed to the previous method involving the non-linear behaviour of control valves.

The same electrical analogy is applied as before, there is a parallel between heat transfers and electrical currents. The thermal balance is equivalent to the electrical current equations at the corresponding node.[8] The method can reduced so dramatically whilst still retaining accuracy because the temperatures within walls are not required. The focus is on conduction in walls which are represented by a 3R4C model. The electrical analogy of the conduction heat transfers is represented the same way as the common 2R1C building block of LPMs.

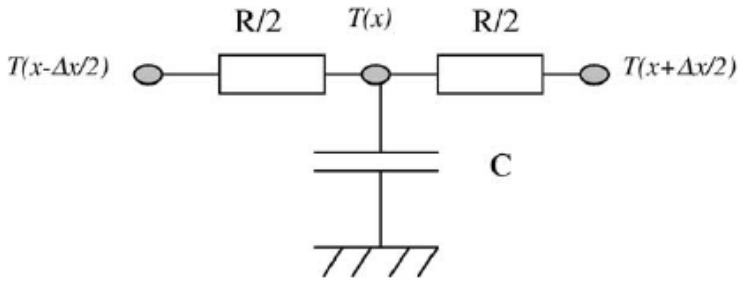

Figure 4: A 2R1C network.

Convective heat flow exchange and long wave irradiative exchanges between surfaces are also included in the resistor and capacitor values. As opposed to Gouda's theory [7], it is only the irradiative effect of the walls to the external environment that is considered and not vice versa. Inside the room the irradiative flow between walls is assumed to be linear.

When applying the method to a building the resistor and capacitor values are calculated according to the thermophysical characteristics of the wall. Each layer can be suitably

transformed into a 3R2C network. [8] This method is used as a reference solution against which the later building models are compared. A new 3R2C network is created and tested for a 0.2m thick, $1m^2$ concrete wall. The 3R2C solution showed closer values to the reference solution than a double 2R1C network. This 3R2C method proves to be accurate and reliable which is why it is used in later studies [9][10] and also in the method for modelling Room 170.

Building models have had difficulty running successful simulations for short time steps however (Fraisse et al)[8] attempt to overcome this problem by creating the 3R4C model. When dealing with short time steps (approx 10 minutes) high frequency inputs need to be included. This is done by considering a thin layer on both sides of the wall. [8] This equates to the addition of two capacitors which take 5% of the thermal capacity from the original two capacitors. The model maintains its simplicity and accuracy. There is the possibility of using the 3R4C method in the reports final model if it is indicated that simulations for short time steps are required. The different methods were tested as a 0.24m thick wall; 0.8m insulating material, 0.16m concrete. The differences of time constants to the reference solution in response to a step change in temperature were as follows 3R2C -1.0%, 3R4C -3.0% and 1R2C -21.5%. The first two models performed well although the 3R4C was slightly disadvantaged as the 5% value was chosen arbitrarily. [8]

2.3.1 Aggregation of Walls and Inclusion of a Heated Floor

The aggregation of walls stems from the transformation of a multi-layered wall to a 3R2C model. The method is derived from the aggregation of several 2R1C models into a single 2R1C model. Once combined into a single 3R2C model, the 3R4C model can be obtained. [8] The aggregation of multiple 2R1C networks works on the principle of maintaining the same time constant when considering any number of walls. The combination of several 3R2C models was tested on a space consisting of a $1m^2$ door and a $1m^2$ wall. The combined result was the average of the two separate temperature step change responses. This shows the method to be accurate.

A heated floor is included in the model to limit any problems of convergence during numerical simulations. A heated floor has a substantial effect on the conditions of the room because of its large surface area. A warmed floor also encourages airflow so the space within the room is more likely to be a uniform temperature. It is possible to model either an electrically heated or a hydraulically heated floor; the electrically heated floor has the heat flow injected onto the heating film whereas the hydraulically heated floor uses a water loop in a steady state.[8] The heating model used is a simpler version of that used in (Gouda et al)[7], this paper uses a steady-state water loop and the effect of the control valve is omitted. The water flow is broken down into three temperatures; the water input temperature, the fluid temperature and the pipe temperature. The fluid heat flow, represented as a 2R1C model, connects to the overall system through two 3R4C models representing the top and bottom surfaces. The simulated heated floor showed a strong correlation with the experimental results.

The final model was integrated within TRNSYS; the program achieved a solution for a thermally homogeneous distribution. The simulation was based upon experimental data from a $95m^2$north-facing classroom in the university.[8] The classroom had a hydraulically heated floor. Using data for the external temperature and the flow injected in the heated floor, the simulation was run over a nine day period and results were sufficiently accurate. Further work suggested in the paper would include the

decomposition of the thermal zone into specific areas attached to the individual components. This report aims to combine the further work suggested by Gouda [7] and Fraisse [8] by monitoring the air temperature stratification through the use of sensors on individual walls. The CFD simulation will include casual heat gains from room occupants and electrical appliances.

2.4 The Dominant Layer Model

The theory of LPMs is further developed in (Ramallo-Gonzalez et al)[9] to create a dominant layer LPM. The work still focuses on a second-order LPM made up of 3R2C as seen in Fraisse's methodology [8] but further reduces the network by using the effect of the most thermally influential layer. The method proves its accuracy when validated on four simple and two complex models. The results show the dominant layer approach is accurate and for this reason it will be included in the work regarding Room 170 if necessary.

Over the past twenty years the simulations for building thermal modelling have become computationally cheaper whilst still retaining accuracy and reducing the time required. When reducing models however, it is only natural that the level of accuracy is reduced. Former simpler simulations used linear dynamic models for the buildings response.[9] The linear models are not capable of modelling radiation and convection and linear approximations are needed if these processes are to be included. [9] RC-networks simplify the thermal modelling of buildings but can still produce large networks. This is because all elements of the building including the individual layers in multi-layered constructions are represented. [9] With the progression to more energy efficient buildings there is the possibility that the cross sections of walls and their materials will become more complex. LPMs dramatically reduce the computational time by reducing the size of the matrices. The work in [6]-[8] documents the process and its benefits. The paper by Ramallo-Gonzalez et al [9] again reduces the size of the matrices to shorten the computational time of simulations.

2.4.1 Defining the Range of Frequencies

The analytical method in [8] reduces multi-layered constructions to systems consisting of three resistors and two capacitors but can be inaccurate for some constructions. The paper [9] focuses not on the transfer coefficients used in other analytical approaches but rather on the range of frequencies generated by the inputs. The reduced model must be accurate under normal operating conditions; this is maintained by limiting the range of frequencies of inputs that affect the system. Boundary conditions in the system are the outside temperature and the internal gains. [9] An upper boundary was defined based on the internal gains; unknown "fast" harmonics were masked by the sampling and deemed irrelevant. [9] This upper bound is also relevant for weather data sampled in an hour. The lower bound is obtained using the physical properties of the construction, in the electrical analogy this is represented as the largest time constant. Previous methods for developing a LPM did take into account the range of frequencies experienced but developed the system properties based on transfer coefficients. For this reason the LPM in (Coley et al)[6] had to be manually set whether to follow or ignore slow trends.

As demonstrated in Gouda's paper [7], there is a lower degree of accuracy in first order models than in second order models, second order models have proved to more accurately model the response while still maintaining a relatively low degree of complexity. [9] Due to the simple wall construction in Room 170 – the walls are a simple brick cross section – the model will itself be first order. The methods described in Ramallo-Gonzalez's paper

[9] for second order models will be applied to the first order model of Room 170. Another possible technique for further development of the project is the dominant layer LPM.

Internal and external gains are cyclic, throughout a cycle the different layers will have different levels of influence on the internal environment. The heavy weight layers have a much larger contribution to the dynamic response of the construction. Through the wall cross-section from inside to outside, there will be a layer of material that stores and releases the most thermal energy. This is the dominant layer. Once identified, all layers before the dominant layer on the internal side are ignored. This reduces the size of the matrices in the LPM. Using the electrical analogy, this is done by making the last capacitor of the LPM the same value as the capacitance as the dominant layer and the resistor of the LPM the same value as the sum of the resistances of the layers between the dominant layer and the inside node. [9]

2.4.2 Validation of the Dominant Layer Model

The method is validated using Bode diagrams for magnitude and phase and is shown to outperform Fraisse's model [8]. An external change of 1°C relates to an internal change of 10^{-5}°C which can be considered negligible. [9] Large differences between the models did occur but these arose at frequencies where the response had been reduced enough to be considered negligible. [9] This shows the advantage of specifying the range of frequencies as operating conditions. The reduced model performed well despite its limitations. Unlike in other papers [6]-[8], the model in (Ramallo-Gonzalez)[9] is tested for a variety of constructions. The constructions tested were; light, heavy, sandwich 1, sandwich 2, proof and all heavy. The model was also tested for periods of 48 hours in winter, spring and summer. [9] This was done to test the accuracy of the model under different convection and radiation values. Although there will be a narrow range of conditions experienced in Room 170 as it has no external walls, it is still important to define a system that will have a high level of accuracy for yearly cycles if scaled up to include the entire building.

The reduced model in (Ramallo-Gonzalez)[9] will be used since it has a comparable degree of accuracy and is simpler than the method defined in Fraisse's paper[8]. The dominant layer model performs particularly well compared to Fraisse's model when used for constructions with many layers. The model is more flexible since it can include substantial layers of intermediate insulation. [9] This shows that a greater emphasis should be put on simulating the common operational frequencies rather than the transfer coefficients which are unaffected by different frequencies. These specific frequencies play a large part in the building simulation since the conditions are cyclic. [9] Second order linear LPMs are tested in multi-layered construction with up to nine layers proving that they will be more than suitable for simulating the single layer walls around Room 170.

2.5 Further Development of the Dominant Layer Model

A more recent paper by Ramallo Gonzalez, A. P and Eames, M [10] details an alternative approach to their previous paper [9]. Previously, the LPM RC-networks were derived from complex numerical [6][7] or analytical methods [8][9] however in the more recent paper [10] complete RC-networks are reduced to simple LPMs with a few elements using a few simple equations. The LPMs are derived using similar methods to the previous paper [9] in that the focus is on maintaining accuracy for the construction across the range of frequencies of the normal operation. The reduced LPMs are able to accurately represent the full building models and a dynamic thermal model. As in Fraisse's model [8] which

covers the aggregation of multi-layered walls, the paper identifies the loss of accuracy when combining many multi-layered walls with different cross sections.

The methodology of Ramallo-Gonzalez [10] is grounded in the earlier research into LPMs and this theory is continued to be used as it not only provides an intuitive representation of the building thermal elements but also the application of Kirchhoff's laws and state-space formulation for their resolution. [10] This same theory is used for the LPM of Room 170.

2.5.1 Conditions for Accurate Modelling

As well as the reduction in matrix size from using the dominant layer model [9], the model is further reduced by combining the surfaces of the buildings. For the reduced model to accurately represent the complete model one of the conditions that must be met is the steady-state condition. For the input response of the reduced model to match the response of the complete model the sum of the resistors in both systems must be equal.[10] This condition is not required for the capacitance values, including those in the dominant layer model, if the system values are found using the methodology in (Ramallo-Gonzalez)[9]. The second condition to be met is accuracy within the operating frequency range. This was a major problem in papers [6]-[8] when short-term high frequency inputs led to instability and not all slow trends were automatically followed. Ramallo-Gonzalez et al [9] [10] overcome this issue by curtailing the range of frequencies. The daily cycle is the obvious period of time in which the external and internal gains repeat themselves. Oscillations in the 24h period have the greatest effect on the operational conditions. [10] This limits complications as found in (Coley et al)[6] where the slow seasonal trends had a detrimental long term effect on the results.

The new reduced model aims to reduce complete models to 3R2C networks as this is shown in Gouda's results [7] to adequately represent the dynamic response. However, this method includes the method in Ramallo-Gonzalez's earlier paper [9] for incorporating the dominant layer model so that the final LPM is a 3R2C network made up of a 2R1C reduced LPM network coupled with a 1R1C network representing the dominant layer. This is done by giving the second capacitor the value of the capacitance in the dominant layer model and the third resistor is made equal to the total resistance between the dominant layer and the inside node. [10]The resistor values for convection and radiation are added to the model at its terminals. [10]

To reduce computational time the aim is to aggregate as many multi-layered surfaces of the building envelope as possible. This includes the aggregation of walls, the floor and the roof. The multi-layered surfaces are aggregated using the same methodology in (Fraisse et al)[8] to create a single 3R2C model but it is later found in the paper to be more accurate excluding the roof from the 3R2C model.

2.5.2 Time Constants

The time constants are the "signatures" of the models and are the fundamental characteristics which define the model. Whether reducing or expanding the system it is important to maintain the same time constant. This is because the time constant is a combination of the conductance and capacitive properties of a structure. To change either of these values is equivalent to changing the materials in the cross section. In order for the reduced model to match the steady state condition the time constants of both models must be equal. This is why the summation of resistances and capacitances is important. The method in Fraisse's paper [8] makes use of two time constants whereas Ramallo-Gonzalez

[10] expands on this and uses four time constants. The time constants are weighted with the total resistance of each surface to reflect the relative influence of components.

2.5.3 Adding Internal and Light Weight Elements

A new area covered by the paper is the addition of elements representing different components in the interior environment. Up until this point a variety of multi-layered constructions formed of a variety of different materials has been modelled. This produces accurate results that represent the conductive heat transfer however once the thermal energy reaches the interior any further detail is lost and the interior environment is assumed to be linear. Further work stated in (Gouda et al)[7] mentions including the effect of people. The effect of casual heat gains and the accurate modelling of heating systems are in use and do improve the model but these inputs are treated as having an instantaneous effect. Fraisse et al [8] suggested further work to include research into the decompositions of zones within a space and this is currently possible with CFD as seen in other elements of the project.

To further improve the LPM of a building, (Ramallo-Gonzalez et al)[10] include partitions, internal mass and light weight elements into the model. Partitions and heavy internal elements, e.g. furniture modify the thermodynamics of a building by becoming heat buffers. [10] Partitions act as internal walls and depending on the design can have many layers. Unlike the exterior walls partitions are only affected by the internal conditions. The heat buffers not only influence the airflow in the environment but also absorb and emit thermal energy from the internal gains. It is possible for furniture to disrupt convection currents within a room meaning that even once a converged solution has been found there are still areas in the room warmer than others. The absorption of thermal energy from internal gains can produce a smoother temperature variation in a 24h period. This is because energy from the partitions is emitted once the occupants leave meaning that the room cools at a slower rate than if the room had no partitions. This effect is dependent on the cross section of the partition.

For simplicity, the construction of partitions has assumed to be symmetrical. [10] This is aided by the fact that both nodes are in contact with the inside node. Using the two time constants of the system, the model can be reduced to a 1R1C network. Since no current flows through the axis of symmetry, a 2R1C network would have an unused resistor. [10] The principle of maintaining the cumulative value for time constants can be used again to reduce the network to a first order 1R1C branch. [10] This branch is added to the reduced LPM. Light weight elements such as windows are included in the model through the use of summing the resistor values.

2.5.4 The Final LPM with Dominant Layer

The final LPM shown in Figure 1 is the reduced LPM made up of the base block (R_1, R_2, R_3, n_1, n_2, C_1 and C_2) which contains the initial reduced model and the dominant layer model. Outside temperature is represented by a voltage source $T_0(t)$ and the internal gains with a current source $g_i(t)$. Internal partitions form the single branch R_x and C_x, light elements are the single resistor R_b. Nodes n_o and n_i are the outside and inside environments respectively. C_{air} is the thermal mass of air inside the building, $R_{c,o}$ and $R_{c,i}$ are the convective surface resistors for the outside and inside.

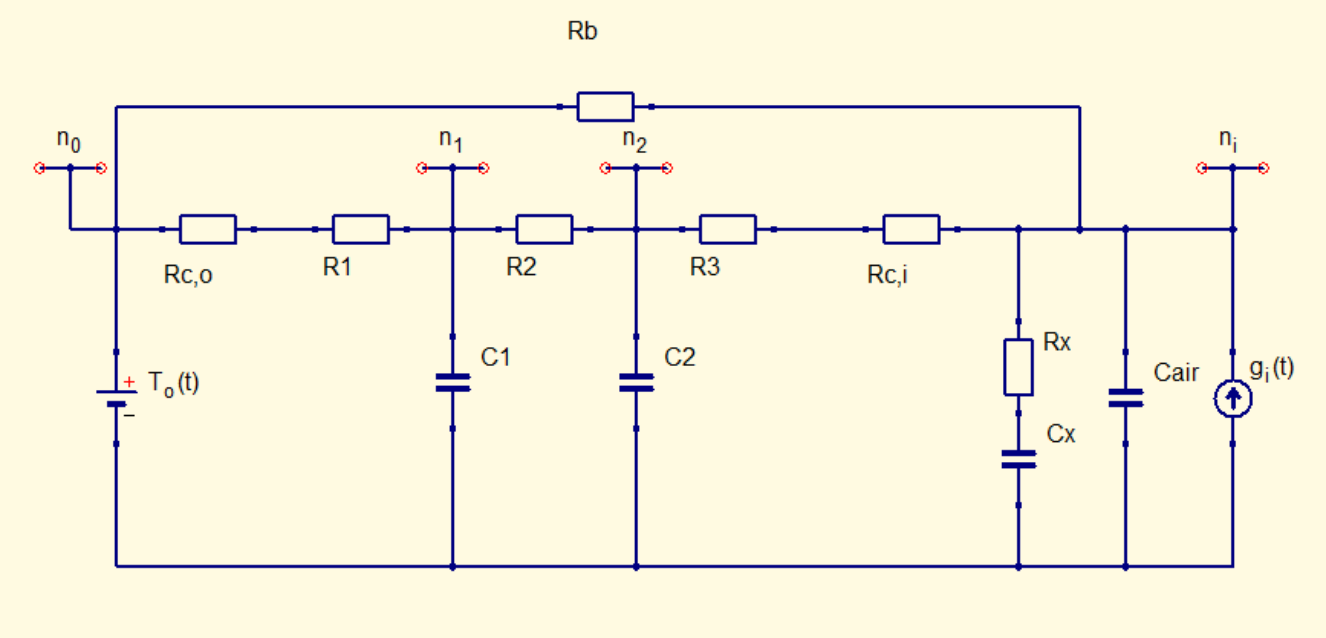

Figure 5: The final LPM in the Ramallo-Gonzalez's later paper.

The final LPM was tested on 500 building designs which covered a range of values for the materials used in the construction of external walls and partitions. The frequency response of both the complete and reduced models was studied to analyse the accuracy of the reduction. [10] The response of the systems was measured in the frequency domain and in the difference of the amplitude and phase of the output to the sinusoidal input. [10] It was shown that the initial loss of accuracy occurred in the reduction of multilayer constructions into 3R2C models. The amplitude fitted well although the phase had a large difference. [10] Another loss of accuracy was reducing several surfaces to a single LPM; this loss of accuracy was substantial. [10] When the building has a uniform construction in all exterior walls, the LPM accurately shows the response in amplitude and acceptable correlation in phase. The LPM systematically underestimates the lag of the outputs. [10]

The LPM generated least accurate results when attempting to reduce multilayer constructions with differing cross sections. Fortunately, most buildings have the same cross section in all external walls and the LPM performs well in this case although the roof needs to be modelled as a separate network. [10] This methodology provides accurate results using simple equations, for this reason this methodology will be used when obtaining a LPM of Room 170 and any further rooms modelled in the project.

3 Theory

3.1 Development of a building model based on an electrical analogy.

The use of an electrical analogy for the construction of a building has been in use for over 70 years. In 1940 Bruckmeyer [11] proposed a method for calculating a single thermal time constant for a single multi-layered building element. [12] This is because RC-networks are able to be built to intuitively represent the thermal response of any construction as the elements share the same properties as the construction components. The components directly relate to the components of the analogy. Looking outside of the engineering perspective, there has also been an economical reason the analogy continues to be used. It provides accurate results from a simple, easily modifiable structure. The process is cost-effective because the analogy can be used for future builds and if the materials are not suitable for energy efficient buildings it costs nothing to change constructions which have yet been built.

The model is based upon T-networks of resistors and capacitors, representing the conductive and storage properties of a wall respectively. The full representation of a multi-layered construction uses one of these T-networks for each of the individual layers. It is important to model each layer as they all have a contribution to the thermal behaviour. The networks of large buildings are large and computationally expensive. The theory of LPMs includes the theory of creating building simulators and the theory of their reduction to lower order networks.

3.1.1 Conduction

Taking any construction into account, all are composed of walls, windows, a roof and a floor. External effects on the building include the weather; temperature, precipitation and wind effects. Internal effects on the building include the effect of the occupants, generating heat and moisture and affecting the internal airflow; HVAC systems by design play a large part and there is also the effect of any electrical appliances in the room(s). Since we are looking at thermal response of the construction effects from precipitation and wind effects can be omitted from the model. The thermal energy within the building is transferred by conduction, convection and radiation. Conduction is by far the most fundamental heat flow process in a building. As recommended in (Matthews et al) [12] model components for the three heat flow processes are modelled separately and later combined.

An assumption present in the LPM is that substances that are characterized by resistance to heat flow have negligible heat capacitance, and that substances that are characterized by heat capacitance have negligible resistance to heat flow. [13]

Theory from (Ogata, K) [13] covers the mathematical modelling of thermal systems. For conduction or convection heat transfer,

$$q = K\Delta\theta \quad (eq.3)$$

Where q = heat flow rate, kcal/sec
$\Delta\theta$ = temperature difference, °C
K = coefficient, kcal/sec °C
The coefficient K is given by

$$K = \frac{kA}{\Delta X} \; for\; conduction \quad (eq.4)$$

Where k = thermal conductivity, W/mK
A = area normal to heat flow, m^2
ΔX = thickness of conductor, m

The thermal resistance R (K/W) for heat transfer between two substances, in this case heat flow through an insulator layer, may be defined as:

$$R = \frac{change\ in\ temperature\ difference,\ K}{change\ in\ heat\ flow\ rate,\ W} \quad (eq.5)$$

The thermal resistance for conduction or convection heat transfer is given by

$$R = \frac{d(\Delta\theta)}{dq} = \frac{1}{K} \quad (eq.6)$$

Massive material layers pose a problem because their heat storage ability cannot be neglected. [12] These layers are modelled by combining both the thermal resistance R and the thermal capacitance C. The thermal capacitance C is defined by

$$C = \frac{change\ in\ heat\ stored, J}{change\ in\ temperature, ℃} \quad (eq.7)$$

Or

$$C = mc \quad (eq.8)$$

Where m = mass of substance considered, kg
c = specific heat of substance, J/kg K

These two values together define the layer, to change either values would be equivalent to changing the layer material. The values are transferred to the T-network of the layer; the thermal resistance is shared equally between the two resistors because the node is at the mid-point of the layer. This can be represented as in Figure 6.

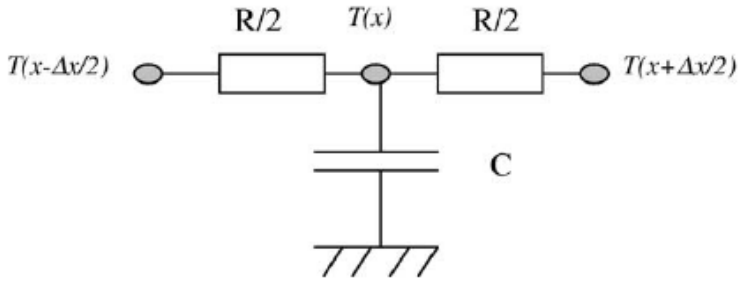

Figure 6: Electrical Analogy of the conduction heat transfers

In the homogeneous layer with low thickness, the conduction equation in discrete form is written as [8]:

$$\frac{T\left(x+\left(\frac{\Delta x}{2}\right),t\right)-T(x,t)}{R/2}-\frac{T(x,t)-T\left(x-\left(\frac{\Delta x}{2}\right),t\right)}{R/2}\approx C\frac{dT(x,t)}{dt} \quad (eq.9)$$

3.1.2 Convection

The second heat transfer process is not as prominent as conduction but still plays a vital part in the thermal model, especially in the internal environment. Convection is needed for the effect of the outside temperature to influence the internal air temperature. Once the thermal energy has diffused through the exterior walls there needs to be a flow of air over the internal surface since conduction cannot take place in a gas. The convection draws the thermal energy off the wall and over time after much circulation the internal air temperature is uniform.

The convective heat flow exchange between a wall surface at temperature T and an air volume at temperature T_a can be expressed with the following Newton equation. [8]

$$\phi_{conv} = h_c A(T - T_a) \quad eq.10$$

Where h_c is the convective heat transfer coefficient, W/m^{2}K
A is the surface area, m^2

The convective resistance is:

$$R_{conv} = \frac{1}{h_c A} \quad (eq.11)$$

The inverse of the convective heat transfer coefficient is the surface resistance, R_{surf}. This value is chosen from a table of values depending on the building component of interest. Using the surface resistance, the convective resistance for a building element with area A can be defined by:

$$R_{conv} = \frac{R_{surf}}{A} \quad (eq.12)$$

Table 1: Surface Resistance Values

Element	Direction	Surface Resistance (m^{2}K/W)
Walls	Horizontal	0.13
Ceiling/Floors	Upwards	0.10
Ceiling/Floors	Downwards	0.17

If necessary, convective resistances can be calculated for the outside and inside surfaces. The resistances are then added to the T-network on either side of the original resistors.

3.1.3 Radiation

The irradiative element of the building construction is included by means of resistance and this is combined with the convective resistors in the T-network. The radiation value is calculated using the Stefan-Boltzmann law. This law states that the total energy radiated per unit surface area of a black body across all wavelengths per unit time, j^*, is directly proportional to the fourth power of the black body's thermodynamic temperature T. [14] The building components are not black bodies since they do not absorb all incident radiation, in this case emissivity, ε is added as a coefficient. The irradiance, j^* (W/m^2) is expressed by:

$$j^* = \varepsilon \sigma T^4 \quad (eq.13)$$

Where ε = emissivity, no units, in this case ε=0.9
σ = Stefan-Boltzmann constant, 5.670400×10^{-8} J/sm^{2}K^4
T = thermodynamic temperature, K

3.2 Integration of Multi-layer constructions

The use of an electrical analogy to model a building is inherently simple but can become rather complex when modelling every internal or external wall. Every element of the building is represented by resistors and capacitors. This becomes even more complex when internal and external walls are composed of many layers to form a multi-layered construction. Since each layer affects the thermal behaviour, each layer is to be included in the model; this can lead to a computationally expensive simulation.

The simulation of a LPM involves the integration of differential equations and summation of matrices. A construction of *n* layers is represented by a RC-network of *n* T-networks, which requires the integration of *n* differential equations. The integration process involves the calculation of an *n x n* matrix of real numbers noted as $e^{A\Delta t}$. [10] To integrate the set of differential equations of a state-space system the time is discretised using a time step and the variables are obtained using: [9]

$$x_{t+\Delta t} = e^{A\Delta t} x_t + Ku \quad (eq.14)$$

Where $x_{t+\Delta t}$ and x_t are vectors of size *n* representing the values of temperatures in the nodes of the system at time steps $t+\Delta t$, Δt is the time step, the $e^{A\Delta t}$ matrix represents the response of the system without inputs, *K* is a *n x 2* matrix that represents the effect of the inputs in the system and *u* is a vector representing the inputs. [10] The vector of variables (x_t) has to be calculated at every time step for the matrix $e^{A\Delta t}$ which only has to be calculated once for a yearly simulation. The matrices *K* and *u* also have to be calculated at every time step. LPMs are widely used because they allow the system matrices to be reduced to a network of a single node. The reduced model must match the complete model's response to inputs; this steady-state condition is met under the equation:

$$\sum_{i,construction} R_i = \sum_{j,LPM} R_j, \quad (eq.15)$$

Where R_i is the resistance of layer *i* in the construction, and R_j represents the resistances of layer *j* in the LPM. [10] Multi-layered constructions play a large role in the size of the system matrices so much research has been conducted focusing on the reduction of systems to a few nodes. [6]-[10] Numerical approaches such as those used in (Coley and Gouda) [6] [7] usually find the best LPM for a system but require the complete network's response in time or frequency. Analytical approaches such as those used in (Fraisse and Mathews) [8][12] use algebraic equations to find the best LPM. [9] The method used in (Fraisse et al) reduces models to 3R2C networks, similarly (Ramallo-Gonzalez et al) use 3R2C networks as the basis to their model but use the theory of (Mathews et al) to aggregate parallel multi-layered surfaces because it uses more time constants to define the network.

3.3 Using T-Networks to Model the Building

The values for all types of heat flow are added to the T-network to represent the single material layer. In the complete building model this T-network may form part of one layer meaning that the multi-layered construction is composed of multiple T-networks connected in series. If a thick layer is represented as only one T-network there is a loss of accuracy. [12] When dealing with a first-order model however these errors need to be managed so that their effect is reduced to a satisfactory level.

In the complete model layers are added by summing the half resistances of adjoining layers. As an example if a two layer model (3R2C) were to be reduced to a single T-network (2R1C) the values of R_1, R_2, R_3, C_1 and C_2 would have to undergo a calculation relating them to the new component values R_{os}, R_{is} and C_s.

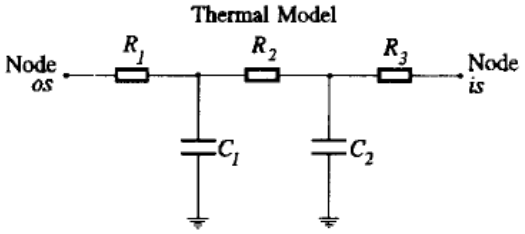

Figure 7: Thermal T-section representation of a two-layered building element.

The method used in (Mathews et al)[12] is the T-matrix. This is a well-known exact solution to solving conduction heat transfer in multi-layered elements. [12] The T-matrix relates the temperatures T (K) and the heat flow q (W) on both sides of a homogeneous slab in the form [12]:

$$\begin{bmatrix} T_{os} \\ q_{os} \end{bmatrix} = \begin{bmatrix} A & B \\ C & D \end{bmatrix} \cdot \begin{bmatrix} T_{is} \\ q_{is} \end{bmatrix} \quad (eq.16)$$

The T-matrix's A, B, C and D represent the thermal properties of the multi-layered element. The subscript *os* describes the outside surface and *is* describes the inside surface. In a general form the T-matrix can represent any number of multi-layered building elements connected in series. The T-matrix of the complete element is the product of the T-matrices of the individual elements in the order in which they appear in the wall: [12]

$$\begin{bmatrix} A & B \\ C & D \end{bmatrix} = \begin{bmatrix} A_1 & B_1 \\ C_1 & D_1 \end{bmatrix} \cdot \begin{bmatrix} A_2 & B_2 \\ C_2 & D_2 \end{bmatrix} \cdots \begin{bmatrix} A_n & B_n \\ C_n & D_n \end{bmatrix} \quad (eq.17)$$

Considering a single T-section (2R1C) as the desired reduced network, the total T-matrix elements can be written as:

$$A = 1 + i\omega R_{os} C_s \quad (eq.18)$$
$$B = (R_{os} + R_{is}) + i\omega R_{os} R_{is} C_s \quad (eq.19)$$
$$C = i\omega C_s \quad (eq.20)$$
$$D = 1 + i\omega R_{is} C_s \quad (eq.21)$$

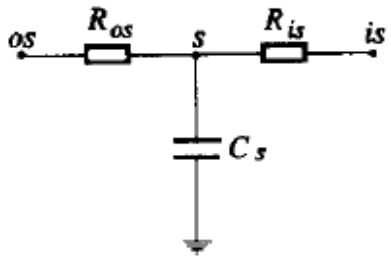

Figure 8: Thermal T-section representation of a multi-layered building element.

It is also important to make use of the frequency (ω (rad/s) and i (i = √-1)) since the external and internal conditions can vary, mostly on a daily cycle. Calculation of the total T-matrix's elements for the representation of a *n*-layered building element produces terms in ω^n. With the example case, a two-layer construction produces terms in ω^2. The inclusion of these higher order terms increases the size of the matrices and greatly increases the computational time. Neglecting these higher-order terms does affect the accuracy of the model but greatly simplifies the system and this is the predominant benefit of a LPM. Omitting the higher-order terms gives the following equations for the T-matrix's elements:

$$A = 1 + i\omega(R_1C_1 + (R_1 + R_2)C_2) \quad (eq.22)$$
$$B = R_1 + R_2 + R_3 + i\omega\big((R_2 + R_3)R_1C_1 + (R_1 + R_2)R_3C_2\big) \quad (eq.23)$$
$$C = i\omega(C_1 + C_2) \quad (eq.24)$$
$$D = 1 + i\omega((R_2 + R_3)C_1 + R_3C_2 \quad (eq.25)$$

By comparing the moduli of the different terms it is possible to determine the effect of neglecting the higher-order terms.[12] For frequency the most important results occur in periods no longer than 24hours. Slower trends in relation to seasonal changes are sometimes desirable however restricting the order of terms in the equation helps to identify interesting trends.

3.3.1 Time Constants

Time constants of the system are important since their value combines the conductive and storage components of a building element; they represent the model's response to an input. The time constants are important for reducing models as the steady state condition has to be met. This means that the response of the reduced model to an input has to be the same as the complete model's response to an input. Two time constants, τ_{os} and τ_{is}, both measured in seconds, can be defined as:

$$\tau_{os} = R_{os}C_s \quad (eq.26)$$
$$\tau_{is} = R_{is}C_s \quad (eq.27)$$

From Figure 8 and by comparing the equations for *A*, it can be seen that the outside surface time constant, τ_{os}, is the sum of the products of the capacitances with the total resistance in the direction of surface *os*. The inside time constant, τ_{is}, seen from comparing the equation for *D* is also the sum of the products of the capacitances but with the total resistance in the direction of *os*. Both equations for *C* show that the single lumped capacitance is given by all the capacitances of all the layers. The steady-state conditions specifies the sums of the

capacitances and resistances in both models must be equal and this is most prevalent in the equations for *B* as the second equation for *B* includes the sum of all the resistors in series.

Once the values for all resistors, capacitors and relevant time constants have been calculated, the values for the reduced 2R1C network are only a few short equations away. In order to find these values the following equations defining the inside and outside surface time constants in terms of the resistance and capacitance of the *jth* layer have to be defined. The *jth* layer is the material layer chosen to be the host for the node in the example case.

$$\tau_{os} = \sum_{j=1}^{n} C_j R_{out,j} \quad (eq.28)$$

$$\tau_{is} = \sum_{j=1}^{n} C_j R_{in,j} \quad (eq.29)$$

$$R_t = \sum_{j=1}^{n} R_j \quad (eq.30)$$

Where C_j is the capacitance of the jth layer, F
$R_{out,j}$ is the resistance on the exterior side of the jth layer, Ohms
$R_{in,j}$ is the resistance on the interior side of the jth layer, Ohms
R_j is the resistance of the jth layer, Ohms
R_t is the total resistance, Ohms

From this is can be shown that the components of the proposed 2R1C thermal T-network are given by:

$$C_s = \frac{\tau_{os} + \tau_{is}}{R_t} = \sum_{j=1}^{n} C_j \quad (eq.31)$$

$$R_{os} = R_i \left(\frac{\tau_{os}}{\tau_{os} + \tau_{is}} \right) \quad (eq.32)$$

$$R_{is} = R_i \left(\frac{\tau_{is}}{\tau_{os} + \tau_{is}} \right) \quad (eq.33)$$

If the reduced model is to be developed for use in a dominant layer model, the frequency of inputs has to be restricted. In this case the time constants for each layer relate to the cut off angular frequencies from the inside and outside nodes. [9]

3.4 Combining Building Elements

The reduction of a multi-layered component to a single 2R1C network reduces the lengthy networks of each element but there is still the need to reduce the network further by combining building elements. This process is made simpler if all building elements are similar in design. In reality there is a variety of different cross-sections depending on the function of the component. The different materials complicate the aggregation procedure but this is dealt with the Dominant Layer Model (DLM) (see Ramallo-Gonzalez et al) [9].

For the combination of building elements two assumptions are made; that the indoor air volume is at a uniform temperature and that the temperature across each surface face is uniform. In reality there is a slight difference with the upper part of the wall warmer than the lower part. This difference is so small however that using the average temperature across the whole face does not lead to a significant loss of accuracy. Similarly the airflow in the room, especially a room occupied by many people, has its own convection currents but uniform temperature is a common assumption in many simulation models. Under these assumptions any number of building elements can be modelled, in this example a thermal model of a building zone with two building elements can be represented by:

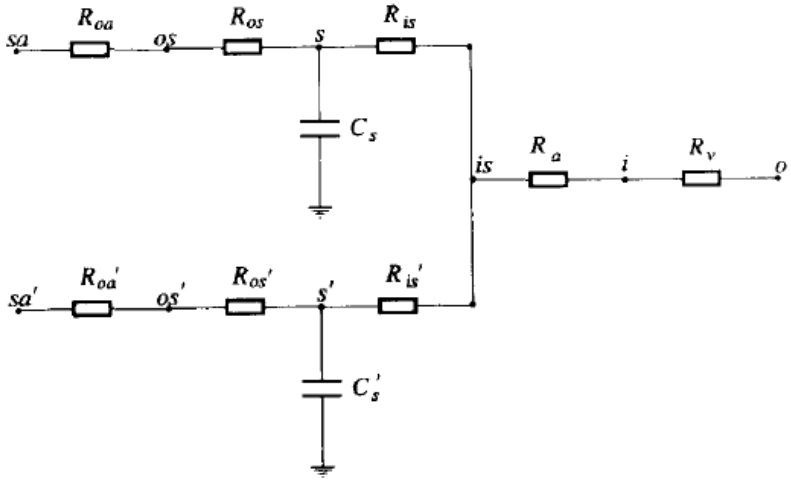

Figure 9: Thermal model of a building zone with isothermal interior surfaces.

The two building elements are represented by heat flow paths between temperature nodes *sa*, the sol-air temperature node representing the external air temperature, and *i*, the uniform indoor air temperature. [12] The second heat flow path is between the second external air temperature node *sa'* and *i*. R_v is the ventilation resistance given by:

$$R_v = \frac{1}{Vol\rho c_p a} \quad (eq.34)$$

Where *Vol*, is the volume of the building zone, m^3
ρ, is the density of air, kg/m^3
c_p, is the specific heat capacity of air, J/kgK
a, is the air change rate per second, l/s

The individual air resistances, R_{ia}, of each building element are replaced by a single indoor air resistance R_a, which is equivalent to all the individual indoor air resistances in parallel. [12] The indoor air resistance of a building containing *m* building elements is given by:

$$R_a = \left[\sum_{k=1}^{m}\left(\frac{1}{R_{ia}}\right)\right]^{-1} \quad (eq.35)$$

3.4.1 The Y-Matrix

A single-order thermal model is achieved by combining the heat paths of the elements into a single heat flow. The methodology of (Mathews et al)[12] does this by utilising the T-

matrix equations for one-dimensional heat flow. A T-matrix equation is determined for each building element quantifying the heat flow from the sol-air temperature node, *sa*, to the indoor surface node. A single Y-matrix for all of the building elements consists of the individual Y-matrices for the admittance of each building element. From this single Y-matrix a single T-section approximation can be found. The example two building element model can then be simplified to a first-order thermal model once the total resistance of the model and the two time constants τ_{os} and τ_{is} are calculated. It is also important to calculate the total steady-state resistance of all the building elements in parallel, R_t, and the remaining two time constants:

$$R_s = \left[\sum_{k=1}^{m}\left(\frac{1}{R_{ia}}\right)\right]^{-1} \quad (eq.36)$$

$$\tau_o = \sum_{k=1}^{m}\left((\tau_{os})_k \cdot \frac{R_s}{(R_t)_k}\right) \quad (eq.37)$$

$$\tau_i = \sum_{k=1}^{m}\left((\tau_{is})_k \cdot \frac{R_s}{(R_t)_k}\right) \quad (eq.38)$$

With these values it is possible to determine the three components of the single T-network that represents the combined building elements. The components are calculated using the same equations for the original T-network except the variables in these equations relate to the sum of the building elements.

$$C = \frac{\tau_o + \tau_i}{R_s} = \sum_{k=1}^{m}\left(\sum_{j=1}^{n} C_{j,k}\right) \quad (eq.39)$$

$$R_o = R_s\left(\frac{\tau_o}{\tau_o + \tau_i}\right) \quad (eq.40)$$

$$R_i = R_s\left(\frac{\tau_i}{\tau_o + \tau_i}\right) \quad (eq.41)$$

3.5 State-space model

The advantage of RC-networks representing buildings is that they can be modelled mathematically by a set of first order differential equations, i.e. state-space systems. [13] A state-space representation is beneficial when dealing with optimal control problems. State-space as defined by (Ogata, K) [13] is the *n*-dimensional space whose coordinate axes consist of the x_1 axis, x_2 axis,..., x_n axis, where x_1, x_2,..., x_n are state variables. Points in state space are able to represent any state.

Using a state-space model, systems with multiple inputs and outputs linear or non-linear can be linearised so that they can be treated equally in state equations and output equations. The method makes use of matrices to represent the state, the input, the output

and the direct transmission. The equations in these matrices are derived from the T-network using Kirchhoff's current laws. In the matrix form the values are updated at each time step to produce each output value. A state-space model of the building space can be written as:

$$\dot{X} = AX + BU \quad (eq.42)$$

$$Y = CX + DU \quad (eq.43)$$

Where X is the state vector $[T_1\ T_2\ T_3\ T_4\ ...\ T_n]^T$, U is the input vector $[U_1\ U_2\ U_3\ U_4\ ...\ U_n]$ and Y is the output vector. This integration of first-order differential equations is performed by circuit simulators. In the case of this project the program used is QUCS (Quite Universal Circuit Simulator).

4 Methodology

4.1 Choosing a room

As a test bed for the accuracy of the system it was important to choose a room that had a simple geometry and experienced minimal affect from external conditions so that the number of variables would be low. The chosen room (Harrison building Room 170) has no exterior walls and a simple stepped seating arrangement. The room was chosen as the sources of largest airflow were restricted to the doors and ceiling inlets and outlets. With no exterior walls the ambient conditions of the room interior were largely unaffected by climate, i.e. the temperature, airflow and humidity are near constant. This was also a beneficial simplification as the absence of windows meant that there was little manual manipulation of the temperature control. The manually opening and closing of windows has proved to be a problem for previous thermal modeling work. [6] Furthermore, the room was rarely used for lectures and this meant there was little restriction on group work or data collection. Dimensions of the room were taken and input into SolidWorks. The model in SolidWorks was used extensively for the individual work of Locci, G and Smith, A [15][16] who developed accurate simulations showing the airflow within the room and the thermal plumes produced by single and multiple occupants.

The heat sources permanently in the room were the computer block at the front of the room; this consists of two desktop hard drives and a monitor, and the projector block at the rear of the room. Normal lecture rooms are equipped with only one projector however Room 170 is the visualisation suite and therefore has an additional two projectors for 3D projection. With only one projector the velocities and temperatures of the convective airflow are small and are susceptible to variation from any other airflow such as draughts. However, the larger heat output from the three projectors combined creates a more pronounced convective flow which is important for calibrating the electrical sensors and the simulation. In all simulations the projectors were treated as one unit for simplicity. Further heat sources include the lights. Work conducted by Smith, A simulated the casual heat gains from a room full of people and Locci, G covered the thermal differences in the airflow and surface temperatures. [15][16] This was also tested under different air conditioning settings. It was found that the difference in surface temperature created by the projector and computer were not more than 1°C under medium and high ventilation rates. [15] This information was used in the LPM for calibration.

4.2 Creating a RC-Network

The RC-network to be created for Room 170 was to be low-order since the aim of using a LPM in the project was to have a computationally inexpensive simulation. It is the inclusion of multi-layered constructions which creates large networks; fortunately since none of the surfaces were exterior walls their construction was simple. All four vertical walls were made of brick, two brick widths thick with a painted surface on both sides. This meant that the vertical walls could automatically be considered as two port networks with two resistors and one capacitor. The floor and ceiling were also able to be modelled simply as 2R1C networks. The ceiling consisted of an acoustic tile hanging ceiling, above this was a 0.86m air gap and the floor of the room above was supported by wooden panels held in place by aluminium I-beams. It was decided that since the size of the air gap was considerably large, it would act as an insulator and nullify any heat flow between Room 170 and the room above. For this reason the ceiling was modeled as a 2R1C network. The floor was covered by a thin carpet layer, on top of a linoleum layer, on top of concrete. The substantial effect of the concrete in comparison to the significantly thinner linoleum and carpet layers meant that only the modeling of the concrete was deemed necessary. Figure 10 shows the top down layout of the rooms adjoining Room 170.

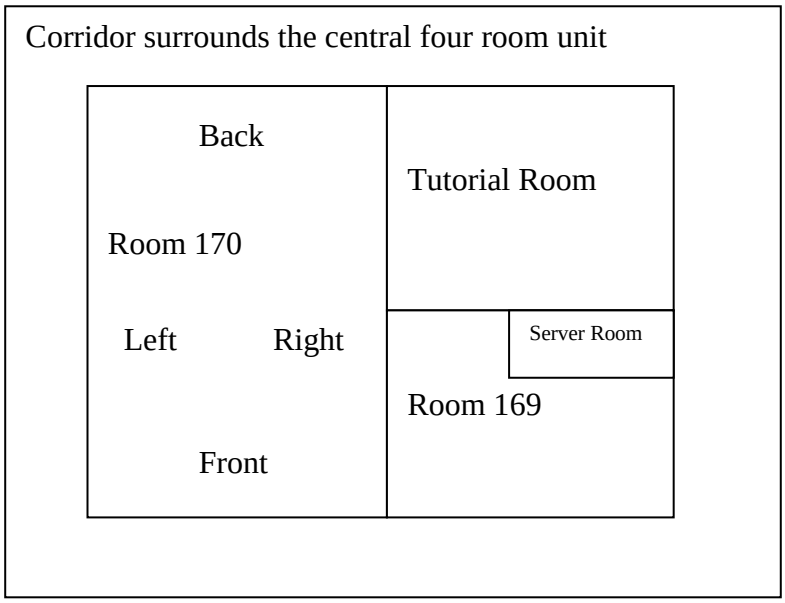

Figure 10: Diagram of Room 170 and the surrounding rooms.

The large walls are labeled “Left” and “Right” and the small walls are labeled “Front” and “Back”. They are all the same construction and thickness. Three of Room 170’s walls are connected to the corridor space. The Right wall is bordered by a tutorial room and Room 169. The server room is connected between the tutorial room and Room 169 but does not border Room 170.

Initially the walls were lumped together as “Large walls” (left and right) and “Small walls” (front and back) this was because the calculations for the combined walls would be equal since the walls were of the same dimensions. It was later decided that it would be more accurate to lump the walls as “Large wall” (front, left and back), “Small wall 1” (the half of “Right” wall adjoining the tutorial room) and “Small wall 2” (the half of “Right” wall adjoining Room 169). This was done to simplify any future works which would include

the effects of more surrounding rooms and eventually the building. By lumping the walls in this manner, any temperature differences between the corridor, the tutorial room and Room 169 would be easier to model.

The final LPM of Room 170:

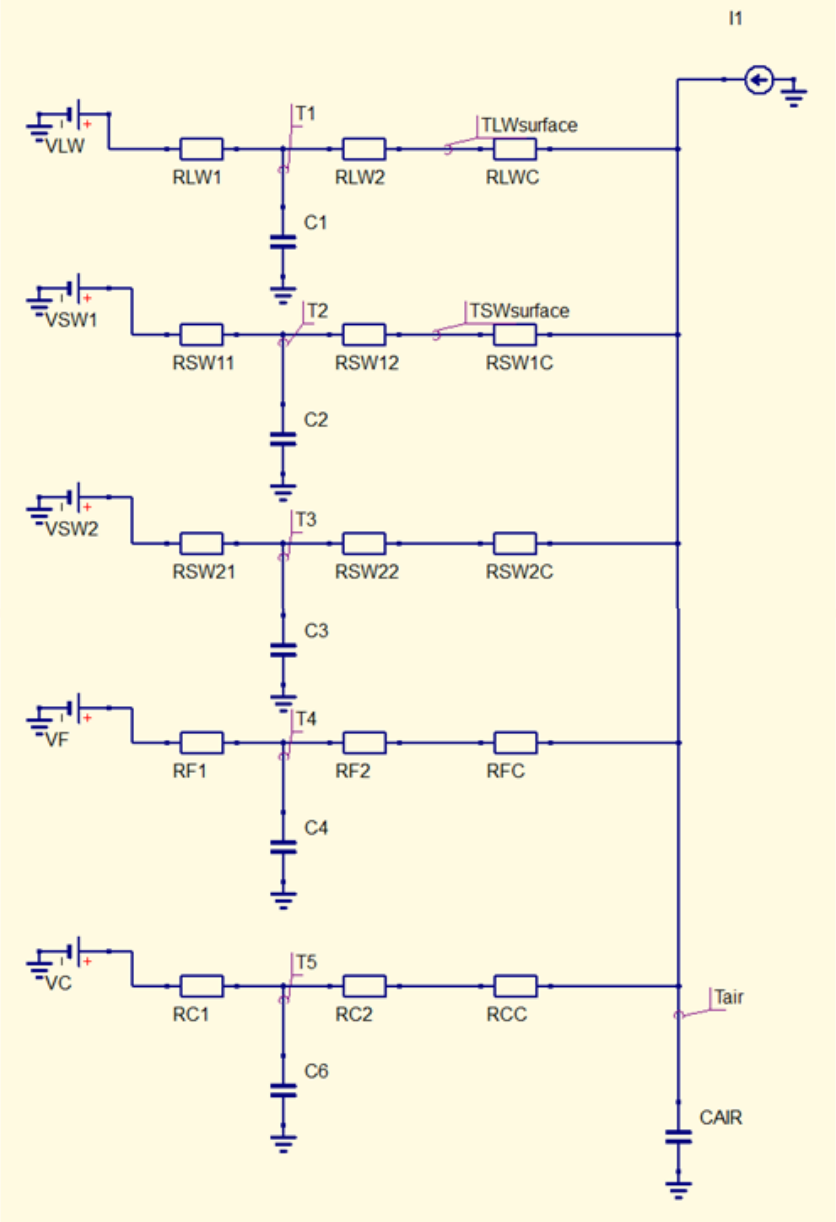

Figure 11: Final LPM for Room 170

The five branches model the surfaces *LW*, Large wall; *SW1*, Small wall 1; *SW2*, Small wall 2; *F*, Floor and *C*, ceiling. The voltage sources on the left are the temperature inputs, the resistors on either side of the nodes *T1-T5* are the element resistances, and the resistors with the suffix *-C* represent surface resistance for each branch. The capacitors *C1 – CAIR* represent the capacitance of the corresponding surface. The current source *I1* represents the heat gain/loss as a result of the ventilation system.

4.3 Deriving the state equations

State equations for the RC-network are derived using the principle of Kirchhoff's current law. The law states that at any node in an electrical circuit, the sum of currents flowing into that node is equal to the sum of the currents flowing out of that node. [17] Using this principle equations were derived for six nodes. Five of the nodes were taken to be at the junction connecting the two resistors and one capacitor on each branch. The sixth node was at the junction connecting the five branches to the current source and the capacitor representing the thermal storage properties of air.

It is important to derive the state equations because the coefficients of the nodes are used in the state space matrices. The state equations define the relationship between the input vector, state vector and output vector. The state equations and state-space model are all automatically derived by the circuit simulator. The state equations from the Room 170 LPM are as follows:

$$C_1\frac{T_1}{dt} = \frac{1}{R_{LW,1}}V_{LW} - \left(\frac{1}{R_{LW,1}} + \frac{1}{R_{LW,2}+R_{LW,C}}\right)T_1 + \frac{1}{R_{LW,2}+R_{LW,C}}T_{AIR} \quad (eq.44)$$

$$C_2\frac{T_2}{dt} = \frac{1}{R_{SW1,1}}V_{SW1} - \left(\frac{1}{R_{SW1,1}} + \frac{1}{R_{SW1,2}+R_{SW1,C}}\right)T_2 + \frac{1}{R_{SW1,2}+R_{SW1,C}}T_{AIR} \quad (eq.45)$$

$$C_3\frac{T_3}{dt} = \frac{1}{R_{SW2,1}}V_{SW2} - \left(\frac{1}{R_{SW2,1}} + \frac{1}{R_{SW2,2}+R_{SW2,C}}\right)T_3 + \frac{1}{R_{SW2,2}+R_{SW2,C}}T_{AIR} \quad (eq.46)$$

$$C_4\frac{T_4}{dt} = \frac{1}{R_{F,1}}V_F - \left(\frac{1}{R_{F,1}} + \frac{1}{R_{F,2}+R_{F,C}}\right)T_4 + \frac{1}{R_{F,2}+R_{F,C}}T_{AIR} \quad (eq.47)$$

$$C_5\frac{T_5}{dt} = \frac{1}{R_{C,1}}V_C - \left(\frac{1}{R_{C,1}} + \frac{1}{R_{C,2}+R_{C,C}}\right)T_5 + \frac{1}{R_{C,2}+R_{C,C}}T_{AIR} \quad (eq.48)$$

$$\begin{aligned} C_{AIR}\frac{T_{AIR}}{dt} = {} & \frac{1}{R_{LW,2}+R_{LW,C}}T_1 + \frac{1}{R_{SW1,2}+R_{SW1,C}}T_2 + \frac{1}{R_{SW2,2}+R_{SW2,C}}T_3 \\ & + \frac{1}{R_{F,2}+R_{F,C}}T_4 + \frac{1}{R_{C,2}+R_{C,C}}T_5 \\ & - \left(\frac{1}{R_{LW,2}+R_{LW,C}} + \frac{1}{R_{SW1,2}+R_{SW1,C}} + \frac{1}{R_{SW2,2}+R_{SW2,C}} + \frac{1}{R_{F,2}+R_{F,C}} \right. \\ & \left. + \frac{1}{R_{C,2}+R_{C,C}}\right)T_{AIR} + I \quad (eq.49) \end{aligned}$$

The coefficients in the state equations were then used for the state-space matrix. The coefficients of $T_1 - T_5$ were the diagonal of matrix "A", the coefficients of T_{AIR} were the final column and the last row consisted of every coefficient in the equation for C_5. Matrix "A" was the matrix to be summed by the state vector "X". Matrix "B" was the matrix to be summed by the input vector "U". For this reason the diagonal of matrix "B" consisted of the coefficients for each voltage source.

$$\dot{T} = \begin{bmatrix} -\frac{1}{C_1}\left(\frac{1}{R_{LW,1}}+\frac{1}{R_{LW,2}+R_{LW,C}}\right) & 0 & 0 & 0 & 0 & \frac{1}{C_1(R_{LW,2}+R_{LW,C})} \\ 0 & -\frac{1}{C_2}\left(\frac{1}{R_{SW1,1}}+\frac{1}{R_{SW1,2}+R_{SW1,C}}\right) & 0 & 0 & 0 & \frac{1}{C_2(R_{SW1,2}+R_{SW1,C})} \\ 0 & 0 & -\frac{1}{C_3}\left(\frac{1}{R_{SW2,1}}+\frac{1}{R_{SW2,2}+R_{SW2,C}}\right) & 0 & 0 & \frac{1}{C_3(R_{SW2,2}+R_{SW2,C})} \\ 0 & 0 & 0 & -\frac{1}{C_4}\left(\frac{1}{R_{F,1}}+\frac{1}{R_{F,2}+R_{F,C}}\right) & 0 & \frac{1}{C_4(R_{F,2}+R_{F,C})} \\ 0 & 0 & 0 & 0 & -\frac{1}{C_5}\left(\frac{1}{R_{C,1}}+\frac{1}{R_{C,2}+R_{C,C}}\right) & \frac{1}{C_5(R_{C,2}+R_{C,C})} \\ \frac{1}{C_{AIR}(R_{LW,2}+R_{LW,C})} & \frac{1}{C_{AIR}(R_{SW1,2}+R_{SW1,C})} & \frac{1}{C_{AIR}(R_{SW2,2}+R_{SW2,C})} & \frac{1}{C_{AIR}(R_{F,2}+R_{F,C})} & \frac{1}{C_{AIR}(R_{C,2}+R_{C,C})} & -\frac{1}{C_{AIR}}\left(\frac{1}{R_{LW,2}+R_{LW,C}}+\frac{1}{R_{SW1,2}+R_{SW1,C}}+\frac{1}{R_{SW2,2}+R_{SW2,C}}+\frac{1}{R_{F,2}+R_{F,C}}+\frac{1}{R_{C,2}+R_{C,C}}\right) \end{bmatrix} \begin{bmatrix} T_1 \\ T_2 \\ T_3 \\ T_4 \\ T_5 \\ V_{AIR} \end{bmatrix}$$

$$+ \begin{bmatrix} \frac{1}{C_1 R_{LW,1}} & 0 & 0 & 0 & 0 & 0 \\ 0 & \frac{1}{C_2 R_{SW1,1}} & 0 & 0 & 0 & 0 \\ 0 & 0 & \frac{1}{C_3 R_{SW2,1}} & 0 & 0 & 0 \\ 0 & 0 & 0 & \frac{1}{C_4 R_{F,1}} & 0 & 0 \\ 0 & 0 & 0 & 0 & \frac{1}{C_5 R_{C,1}} & 0 \\ 0 & 0 & 0 & 0 & 0 & \frac{1}{C_{AIR}} \end{bmatrix} \begin{bmatrix} V_{LW} \\ V_{SW1} \\ V_{SW2} \\ V_F \\ V_C \\ I \end{bmatrix} \quad (eq.50)$$

4.4 Calculating R values

Equation 6 as used in (Ogata, K) [13] calculated the resistance values for conduction as a function of the surface dimensions and thermal conductivity. The walls were defined as "Large wall" (combining Front, Left and Back), "Small wall 1" (half of Right wall) and "Small wall 2" (remaining half of Right wall). The thickness of every wall, ΔX was 0.26m. The thermal conductivity of common brickwork at 25°C is 0.6 – 1.0 W/mK. [18] Since the type of brickwork used in the construction was unknown an average value of 0.8 W/mK was used in the equations.

The ceiling was a covering of 0.0025m thick "Armstrong Ultima acoustic ceiling tile". [19] The thermal conductivity of these tiles is 0.052 W/mK. No information was available regarding the construction of the floor in the Harrison building, from inspection there was a covering of carpet on top of a linoleum layer. Below this is assumed to be concrete. Thermal conductivity of concrete, k = 1.09 W/mK. [20]

The areas of the surfaces were as follows:

- Large wall = 71.35 m^2
- Small wall 1 = 16.005 m^2
- Small wall 2 = 16.005 m^2
- Ceiling = 57.81 m^2
- Floor = 57.81 m^2

Large wall:

$$K = \frac{kA}{\Delta X} = \frac{0.8 \times 71.35}{0.26} = 219.538 \frac{W}{K} \quad (eq.51)$$

$$R = \frac{1}{K} = \frac{1}{219.538} = 0.00456 \frac{K}{W} \quad (eq.52)$$

Small wall 1 and Small wall 2:

$$K = \frac{0.8 \times 16.005}{0.26} = 49.246 \frac{W}{K} \quad (eq.53)$$

$$R = \frac{1}{49.246} = 0.0203 \frac{K}{W} \quad (eq.54)$$

Ceiling:

$$K = \frac{0.052 \times 57.81}{0.025} = 120.25 \frac{W}{K} \quad (eq.55)$$

$$R = \frac{1}{120.25} = 0.00832 \frac{K}{W} \quad (eq.56)$$

Floor:

$$K = \frac{1.09 \times 57.81}{1.0} = 63.013 \frac{W}{K} \quad (eq.57)$$

$$R = \frac{1}{63.013} = 0.0159 \frac{K}{W} \quad (eq.58)$$

The resistance values were split equally between the resistors on either side of the appropriate node. This was because the node is taken to be at the mid-point of the wall.

4.5 Calculating C values

Capacitance values were dependent on the mass of the building element and the specific heat capacity of the material. The greater the mass of the element, the greater the thermal storage capacity. The acoustic tiles had the lowest capacitance values because they were low density and a small volume, the walls had moderate values because although relatively thin, the bricks had a high specific heat. The floor had the largest capacitance value because of the large volume and the high density of the concrete. Although the exact type of brick used in the wall construction was unknown it was most likely to be an engineering brick. Density of engineering brick, ρ = 2165 kg/m^3. [21] Specific heat of common brick, c = 900 J/kgK. [22]

The density of the acoustic tiles was ρ = 5.2 kg/m^2. [19] The specific heat was found to be c = 1340 J/kgK. [20]. The values used for density and specific heat of concrete were ρ = 2880 kg/m^3 and c = 653 J/kgK. [20]

The volumes of the surfaces were as follows:

- Large wall = 18.55 m^3
- Small wall 1 = 4.16 m^3
- Small wall 2 = 4.16 m^3
- Surface area of ceiling = 57.81 m^2. This was used because the density was given as kg/m^2. [19]
- Floor = 57.81 m^3

Large wall:

$$C = Vol\rho c = 18.55 \times 2165 \times 900 = 36{,}144{,}675\frac{J}{kg} \quad (eq.59)$$

Small wall 1 and Small wall 2:

$$C = 4.161 \times 2165 \times 900 = 8{,}107{,}709\frac{J}{kg} \quad (eq.60)$$

Ceiling:

$$C = 57.81 \times 5.2 \times 1340 = 402{,}820\frac{J}{kg} \quad (eq.61)$$

Floor:

$$C = 57.81 \times 2880 \times 653 = 108{,}719{,}798\frac{J}{kg} \quad (eq.62)$$

4.6 Calculating convection resistance values

Convection resistance values were calculated using Equation 12 which takes values for the surface resistance of elements from Table 1.

Large wall:

$$R_{conv} = \frac{R_{surf}}{A} = \frac{0.13}{71.35} = 0.00182\frac{K}{W} \quad (eq.63)$$

Small wall 1 and Small wall 2:

$$R_{conv} = \frac{0.13}{16.005} = 0.00812\frac{K}{W} \quad (eq.64)$$

Ceiling (downwards):

$$R_{conv} = \frac{0.17}{57.81} = 0.00294\,\frac{K}{W} \quad (eq.65)$$

Floor (upwards):

$$R_{conv} = \frac{0.10}{57.81} = 0.00173\,\frac{K}{W} \quad (eq.66)$$

The values for convection resistance were added to the resistors between the second resistor of each branch and the junction connecting the branch to the current source.

4.7 Calculating radiation values

Conduction is the most significant heat flow process in the walls and convection and radiation are the major heat flow processes in the air. The effect of convection is much larger than the effect of radiation. Nevertheless, it was necessary to calculate the resistor values of radiation to decide if the effect was significant to be included in the circuit. The radiation would be most prevalent when the projector had been used constantly during a lecture period. The first set of temperature data taken at various points in the room were recorded immediately after an hour long lecture. The air leaving the projector was at 41°C (314K) this was equivalent to an emissive power of 496 W/m^2.

$$j_p^* = \varepsilon\sigma T^4 = 0.9 \times (5.6704 \times 10^{-8}) \times 314^4 = 496.106\,\frac{W}{m^2} \quad (eq.67)$$

The emissive power of the large wall was also calculated. This was chosen because it was the coldest part of the room with an average temperature of 19.25°C (292.25K). By subtracting the emissive power of the coldest room component from the hottest room component it was possible to quantify the effect of the projector's radiation output.

$$j_{lw}^* = 0.9 \times (5.6704 \times 10^{-8}) \times 292.25^4 = 372.284\,\frac{W}{m^2} \quad (eq.68)$$

$$j_p^* - j_{lw}^* = 123.844\,\frac{W}{m^2} \quad (eq.69)$$

This is the net loss of power from the projector to the large wall per meter squared. By multiplying the value by the area of the large wall it is possible to calculate the irradiative power of the projector on the large wall.

$$\left(j_p^* - j_{lw}^*\right) \times A_{lw} = 123.844 \times 32.01 = 3{,}963.542\,W \approx 4\,kJ \quad (eq.70)$$

The irradiative effect is approximately 4 kJ. A value this low can be considered negligible to the accuracy of the model. Current sources representing irradiative heat gains were not included in the branches of the RC-network.

5 Results

Once the RC-network of Room 170 was completed, the values as calculated in the methodology were input to the appropriate electrical components. The measured surface temperatures were input as voltages for V_{LW} (temperature of large wall), V_{SW1} (temperature of small wall 1), V_{SW2} (temperature of small wall 2), V_F (temperature of floor) and V_C (temperature of ceiling). The temperature in degrees Celsius directly correlates to the voltage in Volts. The current source, *I1* represents the heat gain/loss in the system. The unit Ampere directly correlates to the unit Watt.

5.1 Cases 1 – 4: Results from Experimental Data

Results were generated for four different cases based on the temperature data collected experimentally from the room. The first three cases looked at the conditions in the room with no occupants. The temperatures for the walls and floor were equal and the temperature of the ceiling was marginally higher. Case 1 simulated Room 170 with no occupants, no projector and a medium ventilation rate. Case 2 simulated Room 170 with no occupants, a running projector and a medium ventilations rate. Case 3 simulated Room 170 with no occupants, a running projector and a high ventilation rate. From the results of cases 1-3 the net effect of the projector as a heat source and the warming/cooling effect of the ventilation system could be calculated. The results also helped provide an understanding of the relationship between the ventilation rate, the thermal effect of the projector and the air temperature.

A fourth case was simulated which reflected the conditions used in the Loomans CFD case study method. [16] The building component temperatures were higher than those from Room 170. In this case the room was simulated with 20 occupants, no projector and a medium ventilation rate. This case was used to calibrate the current source value needed to reflect a fully occupied room. Based on these cases it was possible to quantify the current source values needed to reflect the range of possible scenarios. From this a further two cases were simulated. Cases 5 and 6 were predicted thermal models for the hottest scenario (summer and midday) and the coldest scenario (mid-winter and midnight). These simulations showed the future range of air temperatures in Room 170.

Table 2: Results taken from cases 1 - 4.

	Surface Temperatures (V=°C)				
Case	Ceiling, V_C (V)	Walls, V_{SW1}, V_{SW2}(V)	Floor, V_F (V)	Current Source, *I1* (A)	Air Temperature, V_{AIR} (V)
1	21.4	20.2	20.2	-105.0	20.20
2	21.4	20.2	20.2	7.0	20.50
3	21.4	20.2	20.2	-555.0	19.00
4	22.9	23.0	22.4	-105.0	22.60

For cases 1-3 the surface temperatures used were from the Room 170 CFD model which had been based on the experimental data. The average air temperature was calculated from the CFD model. In case 1 the walls and floor were at the same temperature, the ceiling was 1.2°C warmer than the remaining surfaces because of the heat gains from the lights.

Temperature readings at the lights gave an average temperature of T=22.55°C. The CFD simulation was run until the residuals converged, in terms of airflow this meant that the CFD simulation kept running until the convection currents had fully developed. The converged average temperature was 20.20°C. Using this data the value of the current source was increased or decreased until the average air temperature in the LPM met that of the CFD model.

A value of *I1=-105.0A* was needed to generate the LPM's air temperature T_{air}*=20.20V*. The average temperature per meter squared for the surfaces in cases 1-3 was T_{SA}= 20.517°C/m^2, the result shows that the ventilation system in case 1 withdrew 105W from the system to reduce the air temperature by 0.317°C. *I1*=-105.0A corresponds to the marginal cooling effect of the ventilation system on a medium setting.

Case 2 had the same surface temperatures as case 1 and the added heat gain of a running projector. The projector contributed to heating the local air around the projector. Compared to the previous case it is shown that the projector has a heating effect of 0.3°C subject to medium ventilation rates. Through trial and error it was found that a current source of 7A produced an average air temperature, T_{air} = 20.50°C. The heating effect of the projector cannot be explicitly stated to increase air temperature by 0.3°C in all conditions because the air temperature is heavily dependent on the temperature and flow rates of the HVAC system.

The higher ventilation rate in case 3 however had a cooling effect. The air was circulated at such a rate that the projector had no heating influence and the average air temperature was cooler than the surface temperatures. The current source had to be as low as *I1*=-555.0A to cool the average surface temperature of T_{SA}=20.517°C/m^2 by 1.517°C to T_{AIR}=19.00°C.

In case 4 the simulation included 20 occupants modeled as constant heat sources and the surface temperatures were warmer than in cases 1-3. Even with the increase in the number of heat sources there was an overall heat loss and the average temperature of the room was 22.6°C. This was due to the significant effect of the HVAC system; the cooling of the ventilation system counteracted the additional heating from the occupants. This is to be expected as well designed ventilation system should be able to maintain a specified temperature with any number of occupants. The current source value needed to reduce T_{SA}=22.815°C/m^2 by 0.22°C was *I1*=-105.0A. The same *I1* value reduced the average surface temperature by -0.3°C in case 1. This difference can be considered negligible since the occupants would not be able to distinguish a difference in temperature of 0.1°C.

Using these results for overall temperature change and current source value, a linear relationship was found between them.

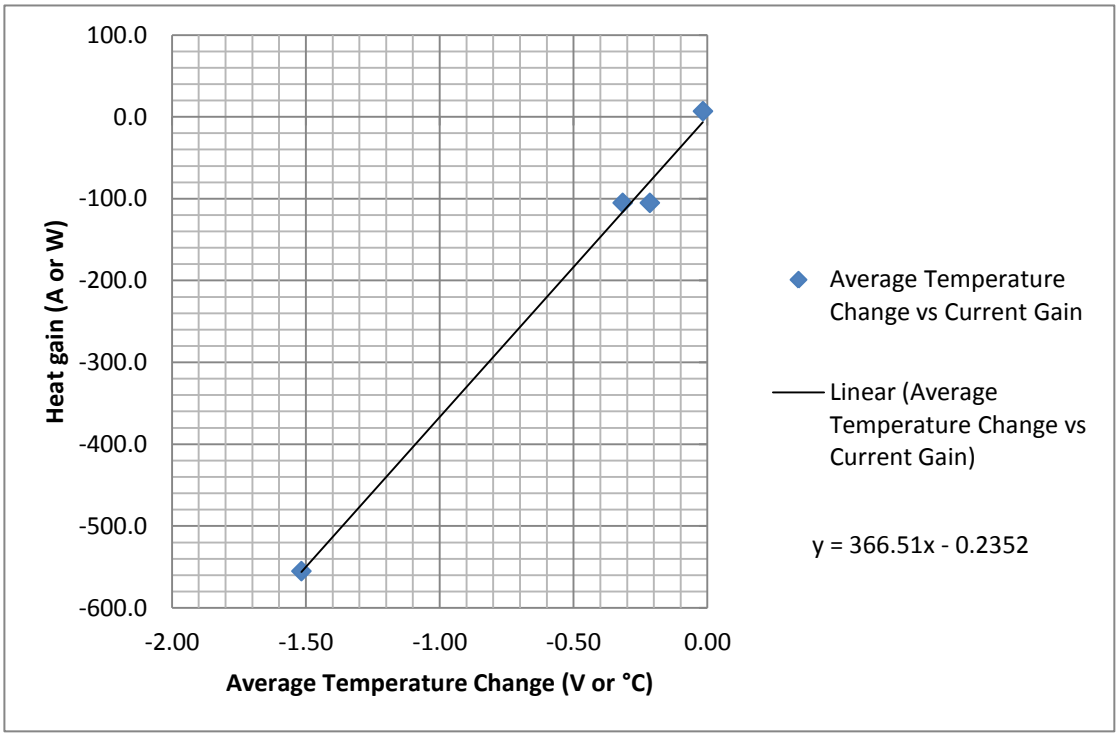

Figure 12: Graph to show the relationship between heat gain and average temperature change.

5.2 Cases 5 – 6: Results from Hypothetical Scenarios

Once the LPM had been calibrated and a relationship derived this was applied to cases 5 and 6 which were designed to test the accuracy of the LPM under the room's most extreme conditions. Cases 5a and 5b were set during summer at midday; 5a having a medium ventilation rate to cool the air temperature by 1.5°C and 5b to cool the air by 4°C. The purpose of 5a was to see if *I1*=-555.0A had the same effect as in case 3 and the purpose of 5b was to test the predicted heat gain value of the equation in the circuit simulator. Cases 6a and 6b were set during winter at midnight; 6a was to test if *I1*=-105.0A lowered T_{SA} by 0.3°C under empty operating conditions as in case 1. Case 6b was used to test the predicted current value needed to raise the temperature by 3°C compared to the value needed in the circuit simulator. The temperatures used for the maximum daytime and minimum nighttime were based on recommendations in "Managing Indoor Air Quality" [23]. The maximum summer daytime surface temperatures were set at 26°C and the minimum nighttime surface temperatures were set at 19°C.

Table 3: Results taken from the cases 5 and 6.

	Surface Temperatures (V=°C)			Air Temperature V_{AIR} (V)	Predicted current gain required *I1* (A)	Actual current gain required *I1* (A)
Case	Ceiling, V_C (V)	Walls, V_{SW1}, V_{SW2}(V)	Floor, V_F (V)			
5a	26.0	26.0	26.0	24.5	-550.0	-560.0
5b	26.0	26.0	26.0	22.0	-1466.3	-1490.0
6a	19.0	19.0	19.0	18.7	-110.2	-110.2
6b	19.0	19.0	19.0	22.0	1099.3	1119.0

In case 5a the predicted current gain required to reduce the average temperature by 1.5°C was 10A higher than the actual gain required in the circuit simulator. When simulated with *I1*=-550.0A, V_{AIR}=24.52V. This difference is small enough to be considered negligible as a change of this degree would go unnoticed by any occupants. According to this result the equation relating heat gain to average temperature change can be considered reliable.

I1=-1466.3A produced $T_{AIR}=22.06V$ but to achieve an absolute value of 22°C the gain needed to be *I1=1490.0A*. The predicted current gain produces an air temperature to within 0.06°C which can again be considered negligible. Between cases 5a and 5b, reliable results for case 5b are more valuable seeing as the need to cool the air temperature to 22°C is more realistic on a summer's day.

The high level of accuracy for the predicted gains is consolidated by the results from cases 6a and 6b. The predicted value for $V_{AIR}=18.7°C$ was accurate to within 0.05°C. This level of accuracy is more than adequate for the thermal model. The predicted values for small changes in average temperature ($\Delta°C<1$) produce results to a higher degree of accuracy than predictions for $\Delta°C>1$. This implies that the gradient of the line equation is marginally too shallow i.e. the error is greater at the ends of the operating range. There is also the possibility that the relationship is not linear. The results from case 6b show that to produce an increase in temperature of 3°C requires a greater magnitude of positive gain than the magnitude of negative gain required decreasing the air temperature by 4°C.

The results from cases 5 and 6 confirm the high level of accuracy in the equation to show the relationship between the heat gain and the average temperature change. Further measurements of different environmental conditions are required from the custom sensors to be built for this project to refine the heat gain equation. It is especially important to take measurements at the upper and lower ranges of the temperature scale controlled by the HVAC system as the relationship is likely to be non-linear in these regions.

5.3 Expanding the Model

The next stage to improving the LPM is to expand the network to not just include Room 170 but also the three connected rooms. The three connected rooms; tutorial room, Room 169 and the server room are all bordered by the same corridor passageway that surrounds three of Room 170's walls. If the four rooms were connected the network would represent the "island" formed by all of these rooms.

Adding a branch to include the tutorial room would be a relatively simple expansion. The tutorial room performs the same functions as the lecture room, Room 170. Heat gains in the room include; lighting, a projector and a computer. The walls are also constructed in the same way; a simple double brick layer. An RC-network of the tutorial room would therefore be almost identical to that of Room 170. Resistor and capacitor values would be smaller because the walls have smaller surface areas and as a result, a lower mass.

The server room would have the lowest resistor and capacitor values because it is the smallest room. As the name suggests it contains a lot of electrical equipment and without the room's HVAC installation there would be huge heat gains. Room 169 is a computer room with nine desktop computers and a single server block. The heat gain/loss values deduced from the

calibration of the Room 170 LPM could be used to model the high ventilation rates present in the server room and room 169.

5.4 Expanding the Model to include the Building

The expansion of the model to include the entire engineering building would be complex. The model would have to take into account multi-layered constructions with different cross sections. The model would need to include the simple double brick layer walls as seen in Room 170 and the multi-layered exterior walls which include several layers of insulation. As mentioned in (Fraisse et al)[8] there is a large error when reducing multiple constructions of different cross-sections. This is because in the process of aggregating walls the effect of low frequency heat sources is not fully taken into account. In the daily cycle, heat sources of lower frequencies affect the internal temperature much more than higher frequencies because the dense brickwork takes a relatively long time to absorb/emit heat. Within the external wall cross-section, some layers have a greater influence on the thermal performance of the wall than others. Layers with a low thermal capacity such as the layer of paint on the inside have a negligible effect on the internal gains in comparison to the high thermal capacity elements such as concrete pillars.

To model the thermal behavior of multi-layered constructions in a reduced RC-network to a higher degree of accuracy requires a Dominant Layer Model (DLM) as specified in the methodology of Ramallo-Gonzalez [10]. The heavy weight layers within the construction have a large contribution to the dynamic response of the building; this is caused by the cyclic internal gains. From inside to outside there is a layer of material which will store and release the majority of the heat during the repeated cycles. This is the dominant layer. [9] The DLM simplifies the RC-network because all layers before the dominant layer (from inside to outside) are ignored.

For the Room 170 LPM to be converted into a DLM LPM, the range frequencies of the inputs would be taken into account. The DLM outperforms Fraisse's model [8] because it produces similar results from a simpler network. This is possible because the range of frequencies for inputs is restricted to fit a 24hr period. The DLM model uses a 3R2C network; this is formed of a base 2R1C network with a 1R1C attachment to represent the effect of the dominant layer. The inclusion of the dominant layer would be possible because the LPM for Room 170 is formed of 2R1C T-networks.

6 Sustainability

The advantage of LPMs over the complete model alternatives is the huge reduction in computational time. The reduction of a complex 50-node RC-network to a system with 4 nodes reduces the computational time of each time step by a factor of 156. That equates to a reduction of the computational time by 99.36%. The reduction of computational time is also a reduction of computational power. Many different construction configurations could be simulated in the time saved. The opportunity to simulate more constructions allows engineers to try a variety of insulating materials in order to find the most energy efficient.

The use of more energy efficient materials in building construction is important to sustainable engineering. Sustainable engineering can be defined as the creative process of utilizing science and technology, making use of energy and resources at a rate, which does not compromise the integrity of the natural environment, or the ability of future generations to meet their own needs. [24] Engineers have an increasing responsibility to think about the social and environmental impacts of their work. This is prevalent in the building sector where there is a continued push from governments and customers for a lower "carbon footprint". In 2009, buildings accounted for about 43% of all the UK's carbon emissions. [25] Buildings and other developments can also damage the environment, through poor waste management or inefficient use of resources. Building thermal management using LPMs helps design buildings that use less energy and have a lower impact on the environment.

The rising cost of energy is predicted to drive the requirement for low-energy solutions. [10] HVAC systems will be developed to be more energy efficient but there is also the possibility that buildings will be designed with more natural ventilation strategies. Natural ventilation systems are difficult to simulate due to the unpredictability of the variables. Whether a building is designed with a HVAC system, a natural ventilation system or a combination of the systems, the LPM theory can be applied to model the temperature distribution across whole buildings. A LPM could be used to determine the heat flow through the building and the most suitable locations for a particular HVAC or natural ventilation system.

It is crucial to include the other topic areas in this project and their capabilities for sustainable engineering. The CFD simulation of human models in different indoor conditions improves the understanding of the human/environment interaction. By using data collected from custom sensors the data can be input as initial conditions for the CFD simulation which models the flow of air and change in temperature. The overall heat gain from the occupants in turn affects the ventilation settings and the thermal profile of the room. Collectively the project furthers understanding of the human/environment interaction and this is vital for the development of sustainable engineering.

7 Conclusion

The aims of this report were to assess the validity of the LPM theory for the application of a model for a specified room in the engineering building and if necessary create an accurate working model. The continued use and development of the LPM theory in building model confirmed the need to include it in the project. The project was to research the interaction of the human body on the working environment and external conditions and vice versa. The LPM has shown that it is the element needed to bridge the gap between the human and the external environment.

By sourcing a range of research papers on the Lumped Parameter Theory it was possible to combine the theory of Ogata, K; Mathews, E; Fraisse, G and Ramallo-Gonzalez et al. into a single accurate RC-network. The choice of room simplified the creation of an accurate LPM by reducing the effect of the external environment. This proved to be beneficial as the results from the model generated results to a high degree of accuracy, within 0.06°C. The model was able to accurately predict heat gain/losses required at the upper and lower ends of the operating scale.

The lumping of parameters and simple modeling techniques meant that all simulations were completed within a trivial amount of time. This is important when using the LPM in a commercial application. A theory/model is required to produce results to a high degree of accuracy within the shortest time possible and using the least computational power possible. These targets are met in the LPM.

The model combines well with the additional aspects of the project; the human thermal model simulates the human's response and its effect on the local atmosphere, this is transferred to the room CFD model which simulates the distribution of temperatures throughout the room. This data is then directly input to the LPM of Room 170 which links the effect of the human's response to the surrounding walls and beyond. The heat gain equation can be refined using results from inside Room 170 and the adjoining corridor and rooms taken by the custom sensors.

A major advantage of using a LPM for building thermal modeling is the ease of modification, the model can be scaled up to include many rooms or floors while still only requiring a trivial computational time to produce accurate results. This outperforms conventional building thermal modeling methods in financial and time savings. There is also huge scope for the future use of LPMs; the voltage sources can be exchanged for data files which contain the input data for a whole year. It is then possible to run a simulation to represent the temperature changes throughout a complete year with a multitude of different multi-layer constructions.

These data files can also contain data for future weather conditions so the thermal performance of buildings subject to future weather can be assessed. This is a major benefit especially as there is the growing demand for energy efficient buildings. It is a growing responsibility of engineers to design constructions that are not only energy efficient for the time they are built but also for the future conditions they may experience due to climate change.

8 References

[1] Department of Energy and Climate Change, "Impacts of climate change in the UK," 2011. [Online]. Available: http://www.decc.gov.uk/en/content/cms/statistics/climate_stats/impacts_cc/impacts_cc.aspx. [Accessed 26 November 2012].

[2] Global Health Observatory (GHO), "Urban Population Growth," 2011. [Online]. Available: http://www.who.int/gho/urban_health/situation_trends/urban_population_growth_text/en/index.html. [Accessed 26 November 2012].

[3] Y. Zhang, "IESD-Fiala model," 3 May 2012. [Online]. Available: http://www.iesd.dmu.ac.uk/~yzhang/wiki/doku.php?id=software:model:iesd_fiala:introduction. [Accessed 4 April 2013].

[4] P. C. Cropper, T. Yang, M. J. Cook, D. Fiala and R. Yousaf, "Coupling a model of human thermoregulation with computational fluid dynamics for predicting human-environment interaction," Loughborough University, Loughborough, 2009.

[5] J. Bunting, "Individual Report - I1," University of Exeter, Exeter, 2013.

[6] D. A. Coley and J. M. Penman, "Second Order System Identification in the Thermal Response of Real Buildings. Paper II: Recursive Formulation for On-line Building Energy Management and Control," *Building and Environment,* vol. 27, no. 3, pp. 269-277, 1992.

[7] M. Gouda, S. Danaher and C. P. Underwood, "Low-order model for the simulation of a building and its heating system," *Building Services Engineering Research and Technology,* vol. 21, no. 3, pp. 199-208, 2000.

[8] G. Fraisse, C. Viardot, O. Lafabrie and G. Achard, "Development of a simplified and accurate building model based on electrical analogy," *Energy and Buildings,* vol. 34, no. 1, pp. 1017-1031, 2002.

[9] A. P. Ramallo-Gonzalez, M. E. Eames and D. A. Coley, "Lumped parameter models for building thermal modelling: An analytic approach to simplifying complex multi-layered constructions," *Energy and Buildings,* vol. 60, pp. 174-184, 2013.

[10] A. P. Ramallo Gonzalez and M. E. Eames, "Lumped Parameter Models for Building Thermal Modelling," 2013.

[11] F. Bruckmeyer, "The equivalent brickwall," *Gesundheits-Ingenieur,* vol. 63, no. 6, pp. 61-65, 1940.

[12] E. H. Mathews, P. G. Richards and C. Lombard, "A first-order thermal model for building design," *Energy and Buildings,* vol. 21, pp. 133-145, 1994.

[13] K. Ogata, Modern Control Engineering, Tehran: Aeeizh, 2002.

[14] Wikipedia, "Stefan-Boltzmann law," Wikimedia, 18 April 2013. [Online]. Available: http://en.wikipedia.org/wiki/Stefan%E2%80%93Boltzmann_law. [Accessed 23 April 2013].

[15] G. Locci, "CFD Modelling of a Lecture Room and Integration of a Human Body," University of Exeter, Exeter, 2013.

[16] A. Smith, "Numerical and Computational Analysis of the Built Environment," University of Exeter, Exeter, 2013.

[17] Wikipedia, "Kirchhoff's circuit laws," Wikimedia, 26 April 2013. [Online]. Available: https://en.wikipedia.org/wiki/Kirchhoff%27s_circuit_laws. [Accessed 26 April 2013].

[18] E. ToolBox, "Thermal Conductivity of some common Materials and Gases," Engineering Toolbox, 22 April 2013. [Online]. Available: http://www.engineeringtoolbox.com/thermal-conductivity-d_429.html. [Accessed 27 April 2013].

[19] Armstrong, "Data file - Ultima," Armstrong, 27 September 2012. [Online]. Available: http://www.armstrong.co.uk/content2/commclgeu/files/24890.pdf. [Accessed 27 April 2013].

[20] C. Thermoelectric, "Material Properties," Custom Thermoelectric, 9 April 2013. [Online]. Available: http://www.customthermoelectric.com/MaterialProperties.htm. [Accessed 15 April 2013].

[21] E. ToolBox, "Weight of Bricks," Engineering ToolBox, 7 September 2012. [Online]. Available: http://www.engineeringtoolbox.com/bricks-density-d_1777.html. [Accessed 25 April 2013].

[22] E. ToolBox, "Solids - Specific Heats," Engineering ToolBox, 7 September 2012. [Online]. Available: http://www.engineeringtoolbox.com/specific-heat-solids-d_154.html. [Accessed 23 April 2012].

[23] H. E. Burroughs and S. Hanson, "The Thermal Environment," in *Managing Indoor Air Quality*, Lilburn, Fairmont Press, 2011, pp. 149-151.

[24] C. F. C. E. &. L. A. Professionals, "Our Mission," Sustainable Engineering & Design, LLC, 30 April 2013. [Online]. Available: http://www.sustainableengineeringdesign.com/. [Accessed 30 April 2013].

[25] GOV.UK, "Improving the energy efficiency of buildings and using planning to protect the environment," Government Digital Service, 30 April 2013. [Online]. Available: https://www.gov.uk/government/policies/improving-the-energy-efficiency-of-buildings-and-using-planning-to-protect-the-environment. [Accessed 30 April 2013].

9 Appendix

Table 4: Temperature data taken experimentally from Room 170.

	Sample 1		Sample 2	
Location	Thermometer	Probe	Thermometer	Probe
Left Wall	19.0	19.5	19.0	20.1
Right Wall	20.0	20.0	19.8	20.3
Front Wall	not taken	20.0	not taken	20.0
Back Wall	not taken	20.0	not taken	20.0
Computer	19.0	20.0	18.9	20.4
Projector	40.5	41.5	22.0	22.7
Lights	22.0	24.0	21.0	23.2
Ventilation	16.5	17.5	18.5	18.5

Table 5: Average temperature change for cases 1-6b

Case	Average Temp.(°C)	Temp. Change (°C)
1	20.517	-0.32
2	20.517	-0.02
3	20.517	-1.52
4	22.815	-0.22
5a	26.000	0.00
5b	26.000	0.02
6a	19.000	0.00
6b	19.000	0.01